Energy 285 (2023) 129490

Contents lists available at ScienceDirect

Energy

journal homepage: www.elsevier.com/locate/energy

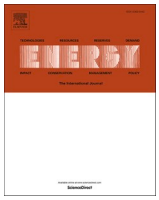

# Optimized siting and sizing of distribution-network-connected battery energy storage system providing flexibility services for system operators

Hosna Khajeh *, Chethan Parthasarathy, Elahe Doroudchi, Hannu Laaksonen

*School of Technology and Innovations, Flexible Energy Resources, University of Vaasa, 65100, Vaasa, Finland*

ARTICLE INFO

Handling Editor: Neven Duic

ABSTRACT

This paper develops a two-stage model to site and size a battery energy storage system in a distribution network. The purpose of the battery energy storage system is to provide local flexibility services for the distribution system operator and frequency containment reserve for normal operation (FCR-N) for the transmission system operator. In the first stage, the priority is to fulfil the flexibility needs of the distribution system operator by managing congestions or interruptions of supply in the local network. Thus, the first stage allocates the battery to ensure reliable electricity supply in the local distribution network. The minimum required size of the battery is also determined in the first stage. The second stage optimally sizes the battery energy storage system to boost the profit by providing frequency containment reserve for normal operation. The first and second stages both solve stochastic optimization problems to design the battery energy storage system. However, the first stage considers worst-case scenarios while the second stage utilizes the most probable scenarios derived from the historical data. To validate the proposed model, real-world data from the years 2021 and 2022 in Finland are employed. The battery placement is conducted for both the IEEE 33-bus system and a Finnish case study. The profitability of the model is compared across different cases for the Finnish case study. Finally, the paper assesses the impacts of cycle aging on the battery's total profit.

## 1. Introduction

Future power systems will face challenges because of the increasing amount of intermittent renewable-based power. In addition, more uncertain demand is added to the system due to the huge electrification in different sectors such as transportation sectors. On one hand, power system operators require more flexibility to deal with the growing uncertainties arising from renewable distributed energy resources (DER) within the system. On the other hand, they can benefit from the flexibility of DERs and take advantage from their potent flexibility to operate distribution and transmission networks.

### 1.1. Motivation

One highly flexible DER is rapidly controllable battery energy storage system (BESS). The European Association for the Cooperation of Transmission System Operators for Electricity (ENTSO-E) has introduced batteries as fast and versatile resources that are capable of providing ancillary services to both DSOs and TSOs [1]. A BESS, functioning as a flexible energy resource, can provide support for the power system frequency, offer local voltage and congestion management as well as back-up power during supply interruptions at different voltage levels. With the help of a BESS, DSOs can actively control the active and reactive power flows in their network to manage congestions and avoid violation of voltage and thermal limits. Beyond its services for local networks, a BESS can assist TSOs with frequency regulation services. It exhibits the ability to rapidly respond to frequency deviations, enabling participation in frequency service markets for profit. Consequently, both TSOs and DSOs can employ BESSs as flexible energy resources to enhance the efficiency of their network operations.

Nevertheless, thorough ex-ante analyses are required before buying a BESS. The BESS should be sized in a way that the revenue obtained from the BESS must outweigh its capital and operational costs. Besides, the BESS needs to be sited optimally if it aims to help with the operation of the distribution network.

### 1.2. Literature review

The existing literature tried to address BESS citing and sizing with

* Corresponding author.
*E-mail address:* hosna.khajeh@uwasa.fi (H. Khajeh).

https://doi.org/10.1016/j.energy.2023.129490
Received 16 April 2023; Received in revised form 23 October 2023; Accepted 26 October 2023
Available online 31 October 2023

**Nomenclature**

*Abbreviations*

| | |
|---|---|
| BESS | Battery Energy Storage System |
| DSO | Distribution System Operator |
| FCR-N | Frequency Containment Reserve for normal operation |
| PoC | Point of Coupling |
| SOC | State of Charge |
| TSO | Transmission System Operator |

*Sets*

| | |
|---|---|
| $t$ | Timeslot [hour = h] |
| $n$, $n^{'}$ | $cn$ Nodes Candidate node |
| $s$ | Scenario |
| $q$ | 3-min time slot |
| $j$ | Partition used in piece-wise linearization |

***Constants***

| | |
|---|---|
| $N^{BESS}$ | The maximum number of BESSs |
| $E^{cell}$ | Energy capacity of the battery cell [kWh] |
| $I^{max}_{n,n}$ | Maximum permissible current that can flow between $n$ *and* $n^{'}$ [$A^2$] |
| $N^{par}$ | The number of partitions |
| $N^{NL,S1/S2}$ | The number of net loads' clusters in the first/second stage |
| $N^{f+,S2}$ | The number of clusters for positive frequency deviations in the second stage |
| $N^{f-,S2}$ | The number of clusters for negative frequency deviations in the second stage |
| $P^{cell}$ | Rated charging/discharging power of the battery cell [kW] |
| $P^{NL}_{n,t,s}$ | Net load at node $n$ and timeslot $t$ of scenario $s$ [kW] |
| $prob^{S2}_{s}$ | Probability of scenario $s$ of the second stage |
| $Q^{NL}_{n,t,s}$ | Reactive power consumed by the load at node $n$ and timeslot $t$ of scenario $s$ [kVar] |
| $R_{n,n^{'}}$ | The resistance of the line between $n$ *and* $n^{'}$ [Ω] |
| $SOC^{min}$ | BESS minimum SOC |
| $SOC^{max}$ | BESS maximum SOC |
| $v^{min}_{n}$ | Minimum voltage of node $n$ (0.95 Per-unit) |
| $v^{max}_{n}$ | Maximum voltage of node $n$ (1.05 Per-unit) |
| $v^{rated}$ | Rated voltage (1 Per-unit) |
| $X_{n,n^{'}}$ | The reactance of the line between $n$ *and* $n^{'}$ [Ω] |
| $Z_{n,n^{'}}$ | The impedance of the line between $n$ *and* $n^{'}$ [Ω] |
| $\Delta f_{q,t}$ | Frequency deviation in the $q$ timeslot at hour $t$ [Hz] |
| $\Delta f^{up}_{t,s}$ | Mean value of upward frequency deviation at $t$ [Hz] |
| $\Delta f^{up}_{t,s}$ | Mean value of downward frequency deviation at hour $t$ [Hz] |
| $\Delta q$ | 3 min = 1⁄20 hour |
| $\Delta S_{n,n^{'}}$ | Maximum power in the piecewise-linearized power flow [kW] |
| $\Delta t$ | 1 h |
| $\pi^{DCC}$ | Price of daily-based BESS capital cost [€/$kWh$] |
| $\pi^{M\&O}$ | Price of BESS maintenance and operation cost [€/ $kWh$] |
| $\pi^{FCR}_{t}$ | FCR-N price for reserving capacity on the FCR-N day-ahead market [€/$kWh$] |
| $\pi^{reg,up}_{t}$ | Up regulation price [€/$kWh$] |
| $\pi^{reg,down}_{t}$ | Down regulation price [€/$kWh$] |
| $\pi^{da}_{t}$ | Day-ahead spot market price [€/$kWh$] |
| $\pi^{cycle}$ | Price of BESS cycling aging for one cycle [€/$kWh$] |
| $\eta^{ch}$ | BESS charging efficiency |
| $\eta^{dis}$ | BESS discharging efficiency |

*Variables*

| | |
|---|---|
| $Cap^{FCR}_{t,s}$ | Power capacity reserved for FCR-N at timeslot $t$ of scenario $s$ [kW] |
| $E^{BESS}$ | BESS energy capacity [kWh] |
| $P^{up,S1}_{cn,t,s}$ | Activated upward power at node $cn$ and timeslot $t$ of scenario $s$ [kW] |
| $P^{down,S1}_{cn,t,s}$ | Activated downward power at node $cn$ and timeslot $t$ of scenario $s$ [kW] |
| $P^{+}_{n,n^{'},t,s}$ | Active power flowing in a downstream direction from $n$ *to* $n^{'}$, at timeslot $t$ of scenario $s$ [kW] |
| $P^{-}_{n,n^{'},t,s}$ | Active power flowing in an upstream direction from $n$ *to* $n^{'}$, at timeslot $t$ of scenario $s$ [kW] |
| $P^{BESS}$ | BESS rated power [kW] |
| $P^{ch,da}_{n=OBP,t,s}$ | BESS charging power with day-ahead spot market prices at timeslot $t$ of scenario $s$ [kW] |
| $P^{dis,da}_{n=OBP,t,s}$ | BESS discharging power with day-ahead spot market prices at timeslot $t$ of scenario $s$ [kW] |
| $P^{FCR-up}_{n=OBP,t,s}$ | BESS activation power in the upward direction at timeslot $t$ of scenario $s$ [kW] |
| $P^{FCR-down}_{n=OBP,t,s}$ | BESS activation power in the downward direction at timeslot $t$ of scenario $s$ [kW] |
| $P^{PoC}_{n=PoC,t,s}$ | Active power coming to the local network through PoC at timeslot $t$ of scenario $s$ [kW] |
| $Q^{PoC}_{n=PoC,t,s}$ | Reactive power coming to the local network through PoC at timeslot $t$ of scenario $s$ [kVar] |
| $Q^{+}_{n,n^{'},t,s}$ | Reactive power flowing in a downstream direction from $n$ *to* $n^{'}$, at timeslot $t$ of scenario $s$ [kVar] |
| $Q^{-,S1}_{n,n^{'},t,s}$ | Reactive power flowing in an upstream direction from $n$ *to* $n^{'}$, at timeslot $t$ of scenario $s$ [kVar] |
| $SOE^{BESS}_{t,s}$ | BESS state of energy at timeslot $t$ of scenario $s$ [kWh] |
| $SI_{n,n^{'},t,s}$ | Auxiliary variable for squared current flowing between $n$ *and* $n^{'}$ at timeslot $t$ of scenario $s$ [$A^2$] |
| $SV_{n,t,s}$ | Auxiliary variable for squared voltage at timeslot $t$ of scenario $s$ [$v^2$] |
| $u^{BESS}_{cn}$ | Binary variable representing if the BESS can be located in candidate node $cn$ |
| $\Delta P_{n,n^{'}j,t,s}$ | Active power flowing between $n$ *and* $n^{'}$ of partition $j$ at timeslot $t$ of scenario $s$ [kW] |
| $\Delta Q_{n,n^{'}j,t,s}$ | Reactive power flowing between $n$ *and* $n^{'}$ of partition $j$ at timeslot $t$ of scenario $s$ [kVar] |

different objectives. Some aimed to address the challenges related to the distribution networks while others focused on the peak shaving and TSO-related services.

Most of the literature proposed to size a BESS to enhance the operation of the distribution network or the local microgrid. They, however, did not consider other profitable services that can be provided by the BESS such as frequency control services. For example, Ref. [2] sized a BESS for PV system owners to invest in buying BESSs. It concluded that not only the BESS assists the DSO and improves the power supply quality in distribution networks, but it also brings profits for the owners. Authors of [3] deployed a two-stage stochastic bi-level programming method to allocate and size a BESS in a deregulated distribution network. In the upper level, the BESS revenue is maximized whereas the lower level clears the distribution market. In Ref. [4], authors proposed

**Table 1**
Comparing the paper with the existing literature that developed planning problems for a BESS.

| Ref. | Site the BESS | Size the BESS | Provide DSO flexibility services | Provide TSO flexibility services |
|---|---|---|---|---|
| [2] | × | ✓ | ✓ | × |
| [3] | ✓ | ✓ | ✓ | × |
| [4] | ✓ | ✓ | ✓ | × |
| [5] | × | ✓ | × | × |
| [6] | ✓ | ✓ | ✓ | × |
| [7] | ✓ | ✓ | ✓ | × |
| [8] | ✓ | ✓ | ✓ | × |
| [9] | ✓ | ✓ | ✓ | × |
| [10] | ✓ | ✓ | ✓ | × |
| [11] | ✓ | ✓ | ✓ | × |
| [12] | × | ✓ | × | × |
| [13] | × | ✓ | × | Frequency response |
| [14] | × | ✓ | × | × |
| [15] | × | ✓ | × | Balance services for a fully standalone system |
| [16] | ✓ | ✓ | × | Transient frequency regulation services and transmission-level services for the network |
| [17] | × | ✓ | × | Frequency regulation service and energy arbitrage |
| [18] | ✓ | ✓ | Peak-shaving for distribution network | Frequency regulation in abnormal conditions |
| [20] | ✓ | ✓ | Supports for operation unbalanced network | Frequency regulation |
| This paper | ✓ | ✓ | ✓ (Voltage and congestion management services) | FCR-N service in normal operations |

to help distribution system planners to allocate a BESS and isolation devices as well as to size the BESS. It aimed to improve the system reliability and boost its revenue by using energy arbitrage. Ref. [5] designed a BESS by solving a security-constrained optimal power flow within a microgrid. The paper proposed to recover the costs of PV forecasting errors by a joint operation of PV-BESS. It stated that the BESS can recoup the PV uncertainty costs under a specific degree of the BESS operation. Authors of [6] identified the optimal BESS placement in a radial distribution network to enhance the reliability of the network. The paper sized the BESS considering the system load and the outage data. In Ref. [7], the authors aimed to mitigate the fluctuations resulting from renewable energy resources and thus increase power reliability and quality. It allocated and sized the BESS to enhance the performance of the distribution network. The objective of the problem was defined to minimize the costs of voltage fluctuations, losses, and peak demand. In Ref. [8], authors proposed a multi-stage model to size a utility-scale BESS. The level of the penetration of dispersed PV panels was assumed to be increasing and the BESS had to accommodate the renewable solar generation in the short-time operation. Similarly [9], tried to allocate a BESS in distribution systems to provide voltage support for the distribution network. A network was assumed to bear a high penetration of PV power. In Ref. [10], the focus was on determining the optimal location and size of a BESS within a distribution network featuring a high number of renewable distributed generations. The objective of the BESS was to mitigate the costs associated with voltage deviations and power losses in the distribution network. Similarly [11], aimed to size the BESS to offer a wide array of flexibility services to the DSO. These services included addressing distribution network outages, non-wires-alternative solutions, and voltage support.

Some other papers focused on other types of services and ignored the effect of BESS on the operation of distribution networks. For instance Ref. [12], developed an interesting work on sizing a BESS in order to reduce the total cost of an extremely fast EV charging station. The sizing objective was to satisfy the station's demand during peak hours, to take advantage of the energy arbitrage and to reduce the total demand charges. Ref. [13] proposed an intelligent approach to size a BESS in a stand-alone microgrid. It also suggested utilizing hybridization sources to improve the frequency responses of the microgrid. In Ref. [14], authors assessed the sizing of a BESS situated in a photovoltaic-equipped energy community. The battery size was determined based on the community's energy consumption and peak demand profiles of households.

Nevertheless, there are a few studies that designed a BESS to provide frequency regulation or other TSO-related services. As examples, In Ref. [15], a BESS was planned to provide energy balance services. The methodology obtains the BESS minimum size to make a fully standalone system. In Ref. [16], authors designed a BESS for post-disturbance situations. The proposed multi-objective problem sites and sizes the BESS to firstly recover post-disturbance line overloads at transmission levels and secondly to arrest frequency excursion. The paper did not consider the BESS revenue obtained from providing these services. Ref. [17] sized a BESS to take advantage of energy arbitrage and provide frequency regulation services. Interestingly, the paper concludes that the BESS should be sized to its highest capacity power when it comes to providing frequency regulation services. Ref. [18] used a heuristic method to determine the optimal BESS placement and capacity in transmission and distribution networks. It performed a sensitivity analysis to allocate the BESS in a transmission network. It then solved power flow and economic dispatch problems to optimally size the BESS. The BESS was considered to minimize peak loads in a distribution network and provide frequency regulation support. In the mentioned literature, the BESS was not tailored to a specific frequency service type [19]. In addition [20], sized and allocated a BESS in a distribution network to provide support for the network as well as frequency regulation services designed for North America. However, frequency regulation services have different capacity market structures and technical requirements, such as activation characteristics and payment methods, which vary from country to country. For the practical application of the sizing problem using real-world data, it is crucial to select the country where the BESS is located. Subsequently, the planning problem can be developed based on the specific regulation service type. In this paper, we assume that the BESS is providing FCR-N service in Finland.

In terms of BESS operation for FCR-N provision, for example [21,22], developed a methodology for the operation of a BESS and electric vehicles to participate in FCR markets, respectively. The main focus was on the BESS and electric vehicle's battery scheduling to meet FCR markets' requirements and how the battery recovers its state of charge (SOC). Ref. [23] proposed bidding strategies for a BESS to participate in FCR capacity markets. Authors of [24] analyzed the operation of a BESS when it participates in FCR provision. According to the paper's results, when the FCR is remunerable, scheduling BESS leads to profits in central European countries. Moreover, the main focus of [25] was on the BESS real-time operation when it provides FCR-N. The aging impacts were also analyzed in that paper. However, these reviewed papers have

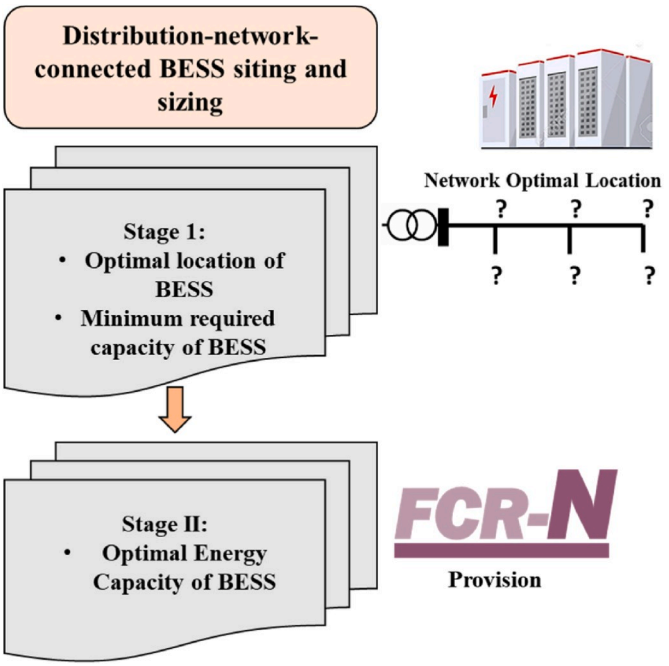


**Fig. 1.** The main architecture of the proposed model.

focused on the operation of the BESS and disregarded its capacity planning and location in the distribution network.

Table 1 provides a comparison between this paper and existing literature that presents models for designing a BESS. The second column indicates whether the paper addressed the issue of BESS allocation. The third column highlights whether the research included an analysis of BESS optimal capacity. In the fourth column, it is indicated whether the studied BESS offered flexibility provision services to the DSO, while the fifth column denotes whether the research explored any forms of TSO-related flexibility.

### 1.3. Contribution and organization

Although the existing literature mainly focused on either DSO- or TSO-related services, this paper sites and sizes a distribution-network-connected BESS for providing both types of flexibility services at the same time. The BESS provides active power support so that the voltages of nodes/buses stay in their permissible range and the power flow constraints are respected. In addition, the proposed method boosts the BESS profit by providing FCR-N services. Currently, FCR-N is one of the profitable services and a suitable option for the BESS since the battery can react in both upward and downward directions, according to the frequency changes [26]. Also, Finnish TSO lists BESS as suitable a technology for providing FCR-N service. To the best of authors' knowledge, there does not exist any study that size the BESS for FCR-N provision. Hence, the main contribution of this paper can be summarized as follows.

1) It develops a two-stage model with two stochastic optimization problems. The first optimization problem allocates the BESS to help the DSO operate the local network in a secure way. The first stage also determines the minimum required size of the BESS. The second stage considers that the BESS is providing FCR-N and aims to determine the BESS size by maximizing its profits.
2) It proposes two different scenario extraction methodologies to develop the first- and second-stage stochastic optimization problems. For the first-stage, worst-case scenarios are extracted to ensure the secure operation of the local network. The second-stage scenarios are selected from the highest-probability scenarios within the historical horizon considered.
3) In the simulation section, the paper compares the BESS optimal size in four cases. It assesses the outcomes if the BESS provides FCR-N and if the BESS works with only day-ahead spot market prices. We use the real-world data of 2021 and 2022 to compare the models together. Finally, the paper analyzes the effects of cycle aging and BESS capacity fade on the profits.

The rest of the paper is organized as follows:

Section 3 provides the detail and the problem formulation of the proposed model. Section 4 introduces the case studies. Section 5 presents the results considering four different cases. Finally, section 6 concludes the paper.

## 2. Problem formulation

This paper considers that a private company owns and designs a specific type of Lithium-ion (Li-ion) BESS. The BESS consists of battery cells as well as other required equipment such as a converter, transformer, and the control system. The BESS is going to be utilized as a service to ensure the secure operation of the local distribution network and provides the DSO with its required flexibility. In addition, it aims to boost the profits by participating in FCR-N markets. In this regard, the BESS planning model has two main goals. First, it should be sited and sized to avoid violation of voltages and thermal limits of the network and secondly, to increase the profits by providing FCR-N services for the TSO. To achieve these two goals, the proposed planning model consists of two stages. The first stage finds the optimal placement of the BESS in the local network. It also determines the minimum charging and discharging power of the BESS to ensure the secure operation of the local network. The second stage, on the other hand, aims to minimize the costs of the BESS while simultaneously providing DSO-related and FCR-N services. Fig. 1 summarizes the main architecture of the paper.

The two-stage methodology offers distinct advantages including distinguishing between the BESS design for DSO- and TSO- related services, the possibility of considering worst-case scenarios to place and size the BESS for the worst-case situations of the distribution network and having the most probable scenarios for the profit maximization purpose of the second stage, and ultimately resulting in the formulation of two optimization problems with fewer dimensions.

### 2.1. Proposed model of lithium-ion battery energy storage system

To develop the BESS model, experimental data from accelerated aging tests on a Li-ion battery cell in laboratory conditions were utilized. More details about the aging tests can be found in Ref. [27]. In the first stage, cell capacity characterization tests were measured in Ah at regular intervals of cycling, in this case at 0, 500, 800, 1200 and 1600 cycles. Then, *Cell Capacity* in Ah was converted to its energy capability in Wh at different cycle intervals, using the following equation:

$$E^{cell}(Cycles) = Cell\ Capacity\ (Cycles) * V_{cell} \quad (1)$$

Where, $V_{cell}$ is the cell voltage in volts. Simultaneously, the rated power of the cell was calculated at 0, 500, 800, 1200, and 1600 cycles. Fig. 2 presents the variations of cell energy and rated power in terms of cycles. Fig. 2 shows how the BESS capacity fade has a non-linear trend. The decreasing slope of the curve becomes steeper when the BESS is more aged. This will also have an impact on the BESS participation in FCR-N market and its profits. The effect will be calculated in section 5.3 of this paper.

To design a BESS, we need to build a battery pack. A battery pack is formulated by multiplying the cell energy capacity by the number of cells in series $N^{series}$ and in parallel $N^{parallel}$. The same equation can be applied for the battery pack's rated power:

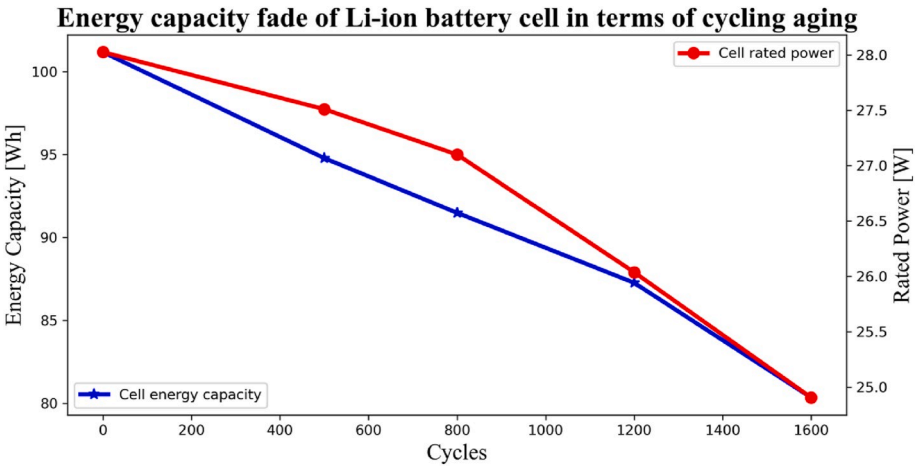


**Fig. 2.** BESS energy capacity face in terms of cycles for our Li-ion BESS.

$$E^{BESS} = N^{series} \times N^{parallel} \times E^{cell} \tag{2}$$

$$P^{BESS} = N^{series} \times N^{parallel} \times P^{cell} \tag{3}$$

Equations (2) and (3) can give us (4), which will be used in the second-stage optimization problem:

$$E^{BESS} = \frac{E^{cell}}{P^{cell}} P^{BESS} \tag{4}$$

### 2.2. Stage I: placement and minimum sizing in distribution network

The first stage optimally places and designs the Li-ion BESS to avoid voltage violations and congestions within its distribution network. This stage is designed to simultaneously handle BESS placement and minimum sizing. We utilize a piecewise-linearized power flow model to obtain the optimal place and minimum flexible power and to check the voltage and current limits of the network. This model has been previously presented in Ref. [28]. If the local network needs upward flexibility at timeslot $t$, the BESS is discharged with power $P^{up,S1}_{n,t,s}$ and if the network asks for downward flexibility at $t$, the BESS is charged with power $P^{down,S1}_{n,t,s}$.

The objective is to find the minimum flexible power that helps operate the network in a secure way [29]:

$$\min_{P^{up,S1}_{cn,t,s}, P^{down,S1}_{cn,t,s}} \sum_t \sum_n P^{up,S1}_{cn,t,s} + P^{down,S1}_{cn,t,s} \tag{5}$$

The constraints associated with the active and reactive power balance are indicated with (6) and (7), respectively:

$$P^{PoC,S1}_{n=PoC,t,s} - P^{NL}_{n,t,s} + P^{up,S1}_{cn,t,s} - P^{down,S1}_{cn,t,s} - \sum_{n'} \begin{pmatrix} P^{+,S1}_{n,n',t,s} - P^{-,S1}_{n,n',t,s} \\ +R_{n,n'} SI^{S1}_{n,n',t,s} \end{pmatrix} + \sum_{n'} \left( P^{+,S1}_{n',n,t,s} - P^{-,S1}_{n',n,t,s} \right) = 0 \forall n,t,s \tag{6}$$

$$Q^{PoC,S1}_{n=poC,t,s} - Q^{NL}_{n,t,s} - \sum_{n'} \begin{pmatrix} Q^{+,S1}_{n,n',t,s} - Q^{-,S1}_{n,n',t,s} \\ +X_{n,n'} SI_{n,n',t,s} \end{pmatrix} + \sum_{n'} \left( Q^{+,s1}_{n',n,t,s} - Q^{-,s1}_{n',n,t,s} \right) = 0 \forall n,t,s \tag{7}$$

The flexible injected/consumed active power of BESS affects balance constraint (6). The balance constraint keeps the balance between the power coming into/leaving the local network at the Point of Coupling (PoC), the net load consumed at each node, the BESS's flexible power at node $n$, and the power flowing through the lines. Correspondingly, (7) ensures the reactive power balance in the local network. The effect of the power flowing through the lines on the voltage of each node is modeled using (8):

$$SV^{S1}_{n,t,s} - SV^{S1}_{n',t,s} - Z^2_{n,n'} SI^{S1}_{n,n',t,s} - 2R_{n,n'} \left( P^{+,S1}_{n,n',t,s} - P^{-,S1}_{n,n',t,s} \right) - 2X_{n,n'} \left( Q^{+,S1}_{n,n',t,s} - Q^{-,S1}_{n,n',t,s} \right) = 0 \forall n,n',t,s \tag{8}$$

Where, the squared voltage and squared current are replaced with two auxiliary variables $SV$ and $SI$ to linearize the model. These two variables should not go beyond the range between their maximum and minimum values, as (9) and (10) state:

$$\left(v^{min}_n\right)^2 \le SV^{S1}_{n,t,s} \le \left(v^{max}_n\right)^2 \forall n,t,s \tag{9}$$

$$\left(I^{min}_{n,n'}\right)^2 \le SI^{S1}_{n,n',t,s} \le \left(I^{max}_{n,n'}\right)^2 \forall n,n',t,s \tag{10}$$

The above constraints limit the active and reactive power flowing through the lines to avoid congestion within the network:

$$P^{+,S1}_{n,n',t,s} + P^{-,S1}_{n,n',t,s} \le v^{rated} I^{max}_{n,n'} \forall n,n',t,s \tag{11}$$

$$Q^{+,S1}_{n,n',t,s} + Q^{-,S1}_{n,n',t,s} \le v^{rated} I^{max}_{n,n'} \forall n,n',t,s \tag{12}$$

Piecewise linearization is applied to the power flow constraints. These constraints are stated below [30]:

$$\left(v^{rated}\right)^2 SI^{S1}_{n,n',t,s} = \sum_j (2j-1) \Delta S_{\boldsymbol{n,n'}} \Delta P^{S1}_{\boldsymbol{n,n'},j,t,s} + \sum_j (2j-1) \Delta S_{\boldsymbol{n,n'}} \Delta Q^{S1}_{\boldsymbol{n,n'},j,t,s} \forall n,n',t,s \tag{13}$$

$$P^{+,S1}_{\boldsymbol{n,n'},t,s} + P^{-,S1}_{\boldsymbol{n,n'},t,s} = \sum_j \Delta P^{S1}_{\boldsymbol{n,n'},j,t,s} \forall n,n',t,s \tag{14}$$

$$Q^{+,S1}_{\boldsymbol{n,n'},t,s} + Q^{-,S1}_{\boldsymbol{n,n'},t,s} = \sum_j \Delta Q^{S1}_{\boldsymbol{n,n'},j,t,s} \forall n,n',t,s \tag{15}$$

$$0 \le \Delta P^{S1}_{\boldsymbol{n,n'},j,t,s} \le \Delta S_{\boldsymbol{n,n'}} \forall n,j,n',t,s \tag{16}$$

$$0 \le \Delta Q^{S1}_{\boldsymbol{n,n'},j,t,s} \le \Delta S_{\boldsymbol{n,n'}} \forall n,j,n',t,s \tag{17}$$

$$\Delta S_{\boldsymbol{n,n'}} = \frac{v^{rated} I^{max}_{\boldsymbol{n,n'}}}{N^{par}} \forall n,n',t,s \tag{18}$$

The following constraints determine the optimal BESS's place (OBP)

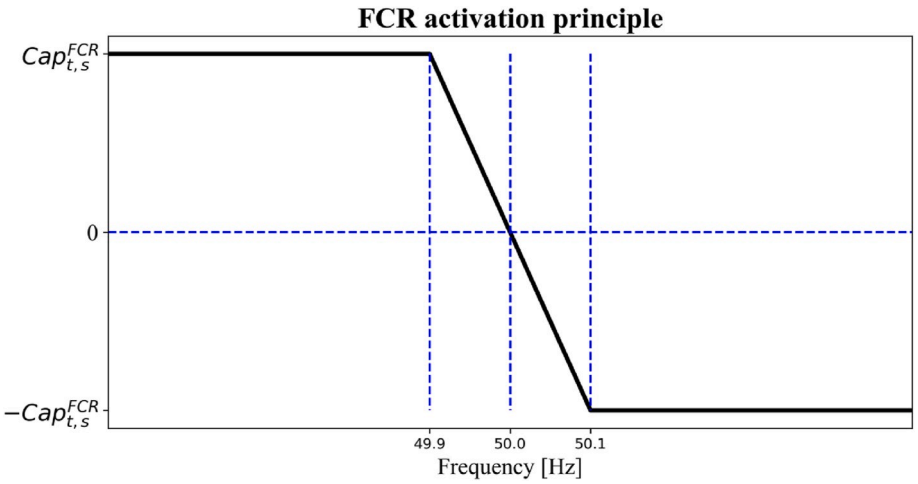


**Fig. 3.** Activation of FCR-N active power capacity according to the system frequency.

which is chosen among candidate nodes (cn):

$$P_{cn,t,s}^{up,S1} \leq Mu_{cn}^{BESS} \forall cn, t, s \tag{19}$$

$$P_{cn,t,s}^{down,S1} \leq Mu_{cn}^{BESS} \forall cn, t, s \tag{20}$$

$$\sum_{cn} u_{cn}^{BESS} \leq N^{BESS} \tag{21}$$

Where, $M$ is a large number. Constraints (19), (20) and (21) indicate that the flexible power should be injected/consumed only at BESS-located nodes. The binary variable $u_{cn}^{BESS}$ equals one for the optimal nodes at which the BESSs are going to be located. The other nodes, on the other hand, have a zero $u_{cn}^{BESS}$. The maximum number of BESSs, i.e., $N^{BESS}$, is assumed to be a parameter that was predefined by the BESS designers.

In addition, the below constraints specify positive variables:

$$P_{cn,t,s}^{up,S1}, P_{cn,t,s}^{down,S1}, P_{n,n',t,s}^{+,S1}, P_{n,n',t,s}^{-,S1}, Q_{n,n',t,s}^{+,S1}, Q_{n,n',t,s}^{-,S1}, \Delta P_{\boldsymbol{n},\boldsymbol{n}',j,t,s}^{S1}, \Delta Q_{\boldsymbol{n},\boldsymbol{n}',j,t,s}^{S1} \geq 0 \tag{22}$$

After solving the minimization problem (5)-(22), the optimal flexible power of the worst-case scenario determines the minimum BESS rated power. The worst-case scenario obtained from the timeslot and scenario in which $P_{cn,t,s}^{up,S1}$ *or* $P_{cn,t,s}^{down,S1}$ are maximum. These optimal values and their maximums are denoted by $P_{n=OBP,t,s}^{up,S1}$, $P_{n=OBP,t,s}^{down,S1}$, $\max(P_{n=OBP,t,s}^{up,S1})$, *and* $\max(P_{n=OBP,t,s}^{down,S1})$, respectively. OBP is the optimal BESS' place that is obtained by solving (5)–(22). Moreover, the BESS' rated power should support both charging and discharging of the BESS. Therefore, minimum rated power of the BESS, $P^{BESS,min,S1}$, yields as follows:

$$P^{BESS,min,S1} = \max\left(\max\left(P_{n=OBP,t,s}^{up,S1}\right), \max\left(P_{n=OBP,t,s}^{down,S1}\right)\right) \tag{23}$$

Finally, the OBP and $P^{BESS,min,S1}$ are sent to the second stage.

### 2.3. Stage II: sizing and cost minimization through FCR-N participation

After receiving the optimal location and minimum rated power of the BESS, the second stage boosts the revenues by providing FCR-N services. This stage aims to find the optimal energy capacity and rated active power $P$ of the BESS that leads to the maximum revenue. Thus, the objective of the second stage minimizes the daily net costs associated with the battery considering different scenarios:

$$\min OF$$

$$OF = \underbrace{\pi^{DCC} E^{BESS}}_{Daily-based\ Capital\ Cost} + \sum_{s} prob_s^{S2} \sum_{t} \Bigg\{ \underbrace{\pi^{M\&O}\left(P_{n=OBP,t,s}^{ch,da} + P_{n=OBP,t,s}^{dis,da} + P_{n=OBP,t,s}^{FCR-up} + P_{n=OBP,t,s}^{FCR-down}\right)}_{M\&O\ Cost} + Cost_{t,s}^{cycle} - \underbrace{\pi_t^{FCR} Cap_{t,s}^{FCR}}_{FCR\ Capacity\ Revenue}$$
$$- \underbrace{\pi_t^{reg,up} P_{n=OBP,t,s}^{FCR-up}}_{Activation\ Revenue} + \underbrace{\pi_t^{reg,down} P_{n=OBP,t,s}^{FCR-down}}_{Activation\ Cost} - \underbrace{\pi_t^{da} P_{n=OBP,t,s}^{dis,da}}_{DA\ Revenue} + \underbrace{\pi_t^{da} P_{n=OBP,t,s}^{ch,da}}_{DA\ Cost} \Bigg\} \Delta t \tag{24}$$

Where the *"Daily − based Capital Cost"* of the BESS is assumed to be a linear function of the BESS's capacity. The *"M&O Cost"* represents the maintenance and operational cost of the BESS which is considered a linear function of the BESS's charging and discharging power. The cycle cost of BESS is denoted by *"*$Cost_{t,s}^{cycle}$*"*. The BESS which is participating in FCR-N markets receives capacity revenue for reserving its capacity, indicated by *"FCR Capacity Revenue"* e. The BESS reserved capacity for FCR is then activated according to the frequency. If the capacity is activated in the upward direction, the BESS is charged and receives revenue, called "*Activation Revenue*". Otherwise, if the activation is downward, the BESS is discharged and incurs costs, called "*Activation Cos t*". This paper considers that in the cases where the BESS is not providing FCR-N, for example when the BESS is being recovered, it can be charged and discharged with day-ahead spot market prices. Hence, The BESS receives revenue, *"DA Revenue"*, based on the day-ahead spot market prices if it is discharged. If the BESS is charged with the day-ahead spot market prices, it should pay *"DA Cost"*.

The cost minimization objective function is constrained by the balance equation:

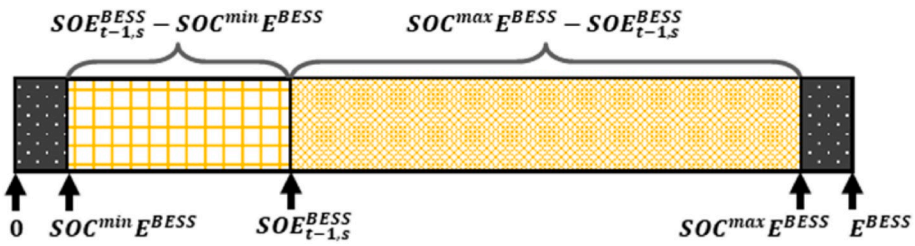


**Fig. 4.** The available BESS state of energy at the beginning of timeslot t.

$$P^{PoC,S2}_{n=PoC,t,s} + P^{FCR-up}_{n=OBP,t,s} - P^{FCR-down}_{n=OBP,t,s} - P^{NL}_{n,t,s} + P^{dis,da}_{n=OBP,t,s} - P^{ch,da}_{n=OBP,t,s} - \sum_{n'}\left(\begin{matrix} P^{+,S2}_{n,n',t,s} - P^{-,S2}_{n,n',t,s} \\ +R_{n,n'}SI^{S2}_{n,n',t,s} \end{matrix}\right) + \sum_{n'}\left(P^{+,S2}_{n',n,t,s} - P^{-,S2}_{n',n,t,s}\right) = 0 \forall n,t,s \quad (25)$$

Where (25) states that the FCR-N downward-activated and the charging power traded with day-ahead prices consume power at the BESS node/bus. Correspondingly, the FCR-N upward-activated and discharging power traded with day-ahead prices inject power into the BESS node. The net load at each node, $P^{NL}_{n,t,s}$, consumes power whereas the power leaves/enters the local network through the PoC node can have both positive and negative values. If $P^{PoC,S2}_{n=PoC,t,s}$ is positive, the power is consumed in the local network while negative $P^{PoC,S2}_{n=PoC,t,s}$ indicates that the power is fed from the local network. It should be highlighted that PoC and OBP are two different nodes unless the first stage determines that the BESS can be put at the PoC. The following constraints restrict the power capacity offered to the FCR-N capacity market:

$$Cap^{FCR}_{t,s} + P^{ch,da}_{n=OBP,t,s} \le P^{BESS} \forall t,s \quad (26)$$

$$Cap^{FCR}_{t,s} + P^{dis,da}_{n=OBP,t,s} \le P^{BESS} \forall t,s \quad (27)$$

The power capacity offered to the FCR-N market plus the power traded with day-ahead prices should not exceed the rated power of the BESS. The FCR-N power capacity should be symmetrical. It means that the BESS needs to submit a power capacity that is able to be activated in both directions, upward and downward directions. Taking into account the downward direction, the FCR-N power capacity and the day-ahead charging power should be lower than the BESS rated power, as denoted by (26). Regarding the upward direction, (27) states that the FCR-N power capacity plus the day-ahead discharging power is upper limited by the rated active power of the BESS.

Equations (28) and (29) relate the upward and downward activated power to the power capacity:

$$P^{FCR-up}_{n=OBP,t,s} = \frac{\Delta f^{up}_{t,s}}{0.1} Cap^{FCR}_{t,s} \forall t,s \quad (28)$$

$$P^{FCR-down}_{n=OBP,t,s} = \frac{\Delta f^{down}_{t,s}}{0.1} Cap^{FCR}_{t,s} \forall t,s \quad (29)$$

The active power capacity of the BESS is submitted to the FCR-N

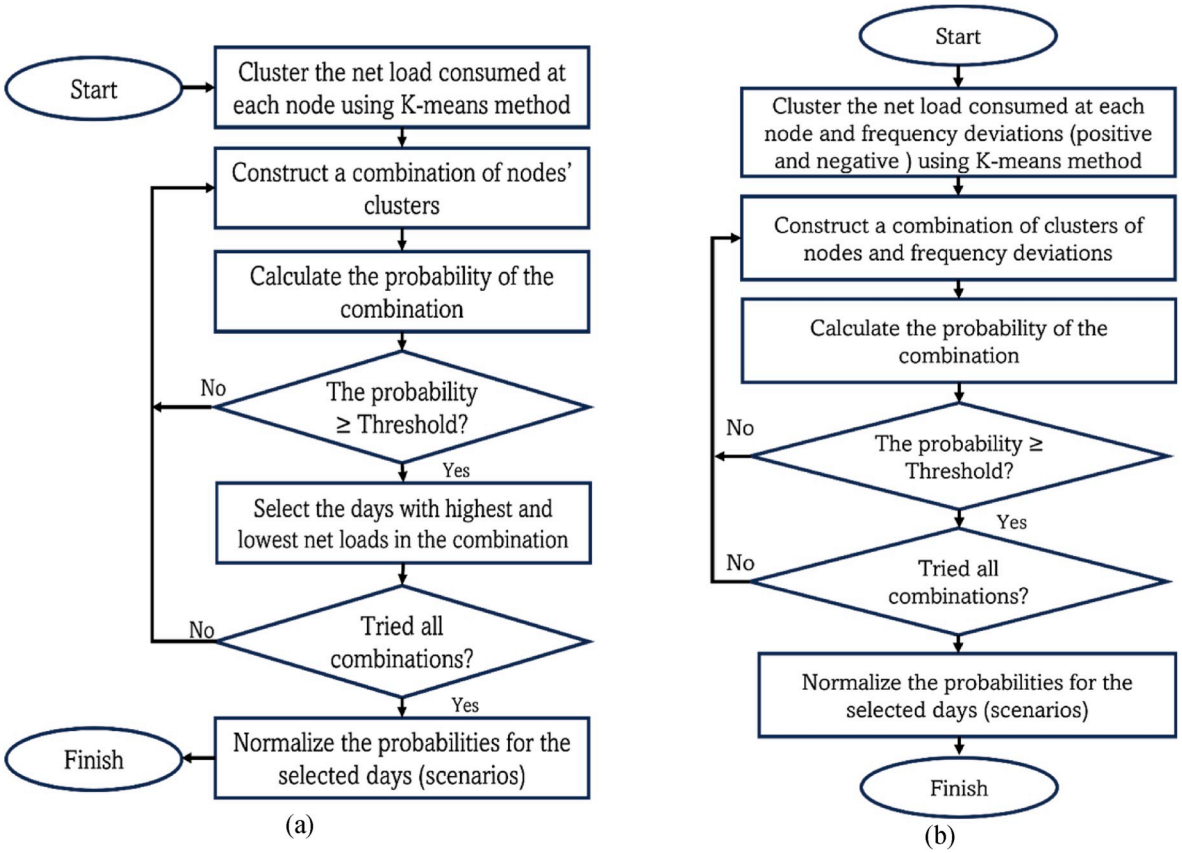


**Fig. 5.** Flowcharts of (a) Algorithm I, first-stage scenario generation & reduction and (b) Algorithm II, second-stage scenario generation & reduction.

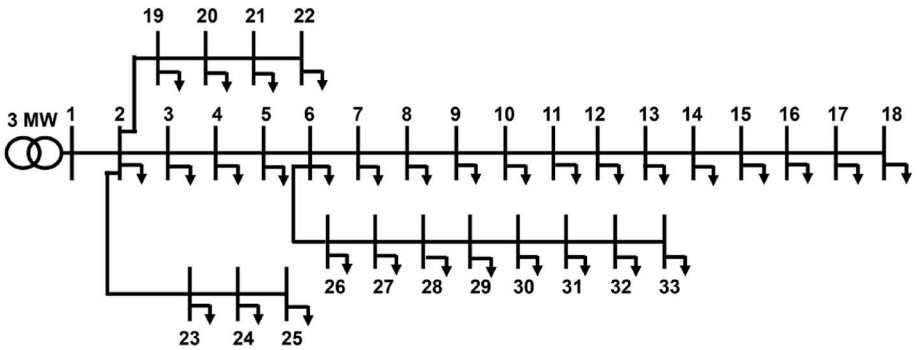


**Fig. 6.** Single diagram schematic of IEEE 33-bus radial distribution system.

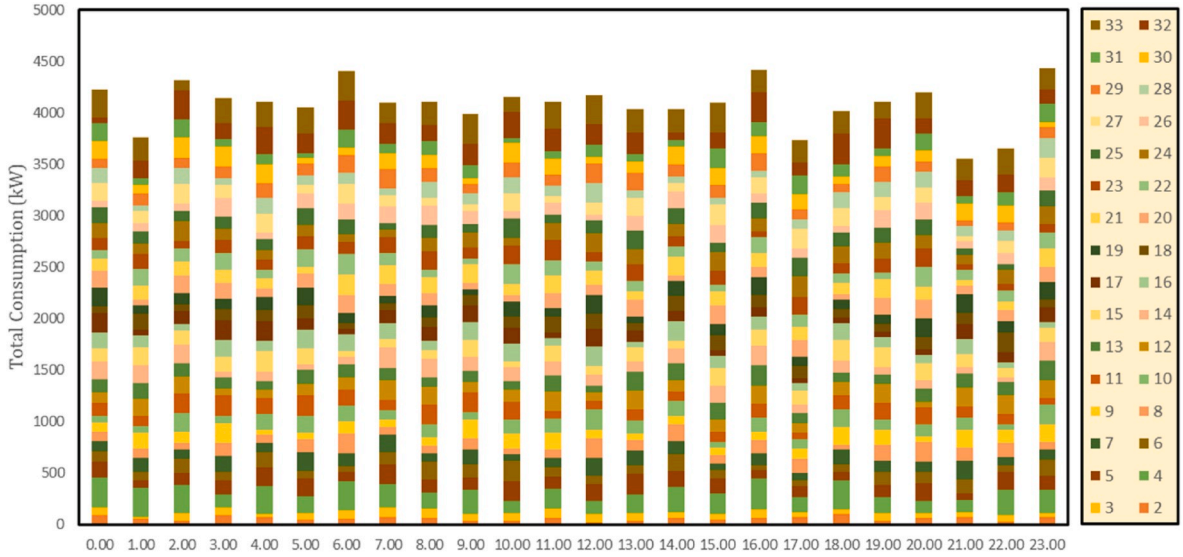


**Fig. 7.** Hourly net load considered for IEEE 33-bus radial distribution system.

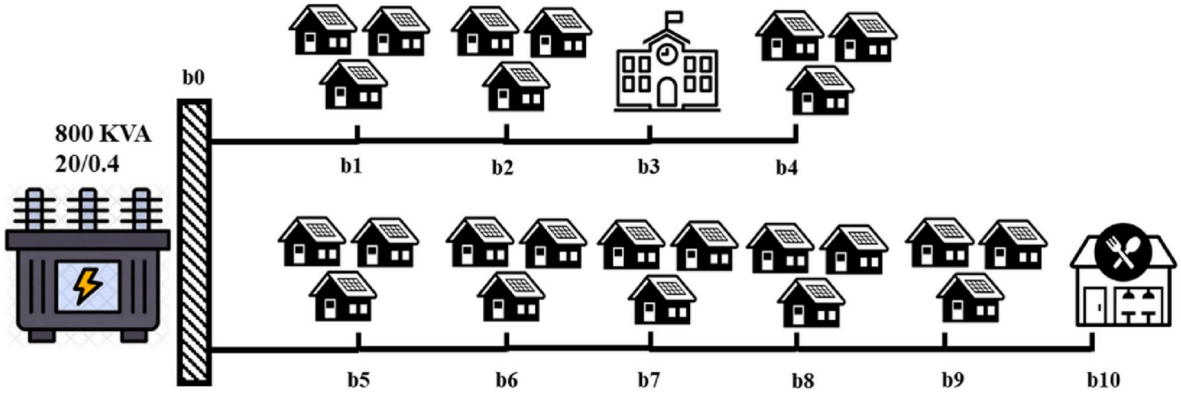


**Fig. 8.** The Finnish local network considered in the paper.

capacity market one day before the actual activation. If the power capacity is accepted, the BESS needs to activate the power capacity according to the frequency. Fig. 3 illustrates the FCR-N activation principle. If the frequency is greater than 50 Hz, the BESS activates in a downward direction. Otherwise, if the frequency is lower than 50 Hz, the BESS activates in an upward direction.

As Fig. 3 shows, the amount of activation should be proportional to the frequency deviation if frequency deviations are lower than 0.1 Hz. Since the paper considers 1-h timeslot, hourly frequency deviations are calculated as follows:

$$\Delta f_t^{up} = \sum_{q=1}^{q=N_q} |\Delta f_{q,t}| \Big| \Delta q \quad if \quad \Delta f_{q,t} \geq 0 \forall t \tag{30}$$

$$\Delta f_t^{down} = \sum_{q=1}^{q=N_q} |\Delta f_{q,t}| \Big| \Delta q \quad if \quad \Delta f_{q,t} < 0 \forall t \tag{31}$$

$$\Delta f_{q,t} = 50 - f_{q,t} \forall t, q \tag{32}$$

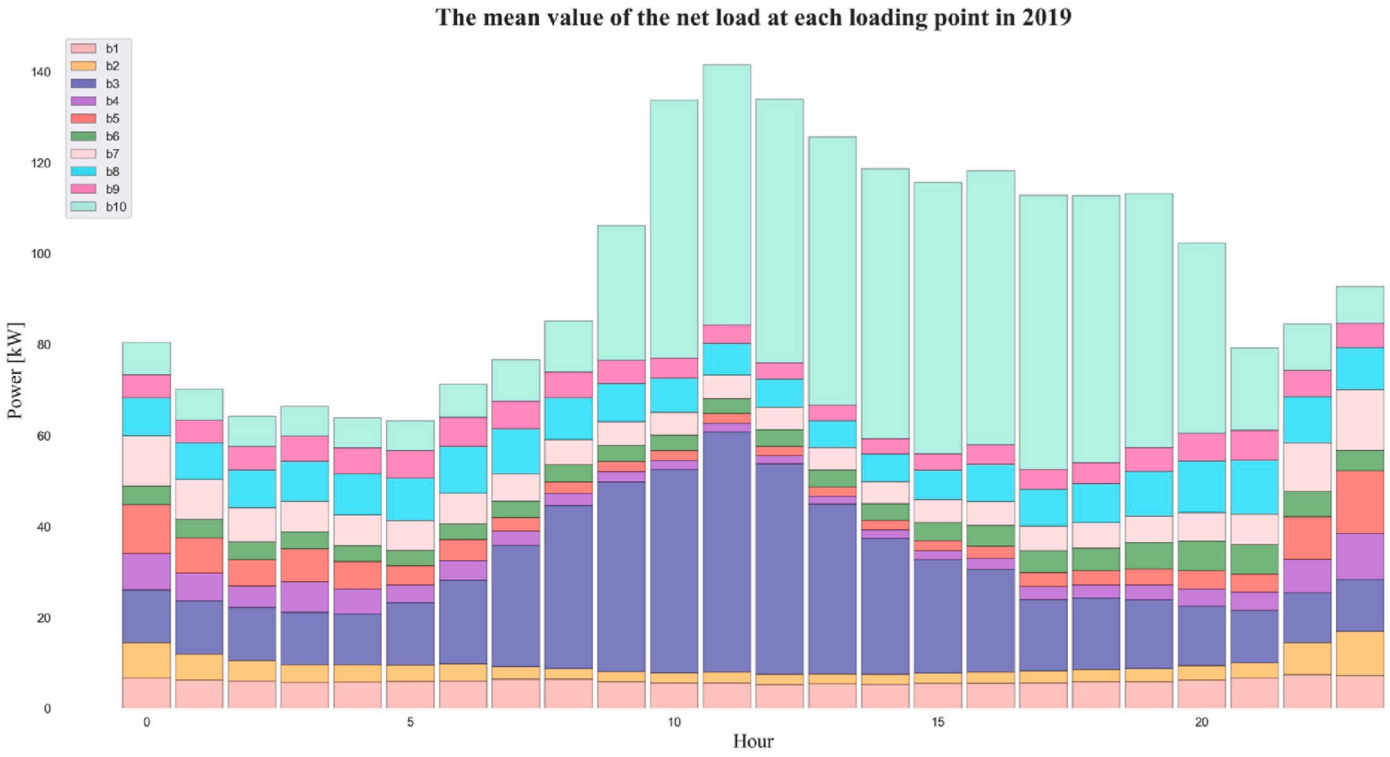


**Fig. 9.** Hourly net loads' mean values considering one year.

**Table 2**
Used BESS parameters.

| $SOC^{min}$ | $SOC^{max}$ | $\eta^{ch}$ / $\eta^{dis}$ | $E^{cell}$ [kW] | $P^{cell}$ [kW] | Cycle life | $\pi^{cycle}$ [€/kWh] | $\pi^{DCC}$ [€/kWh] | $\pi^{M\&O}$ [€/kWh] |
|---|---|---|---|---|---|---|---|---|
| 0.05 | 0.95 | 90 % | 0.1 | 0.028 | 6000 | 0.1 | 0.095 | 0.001 |

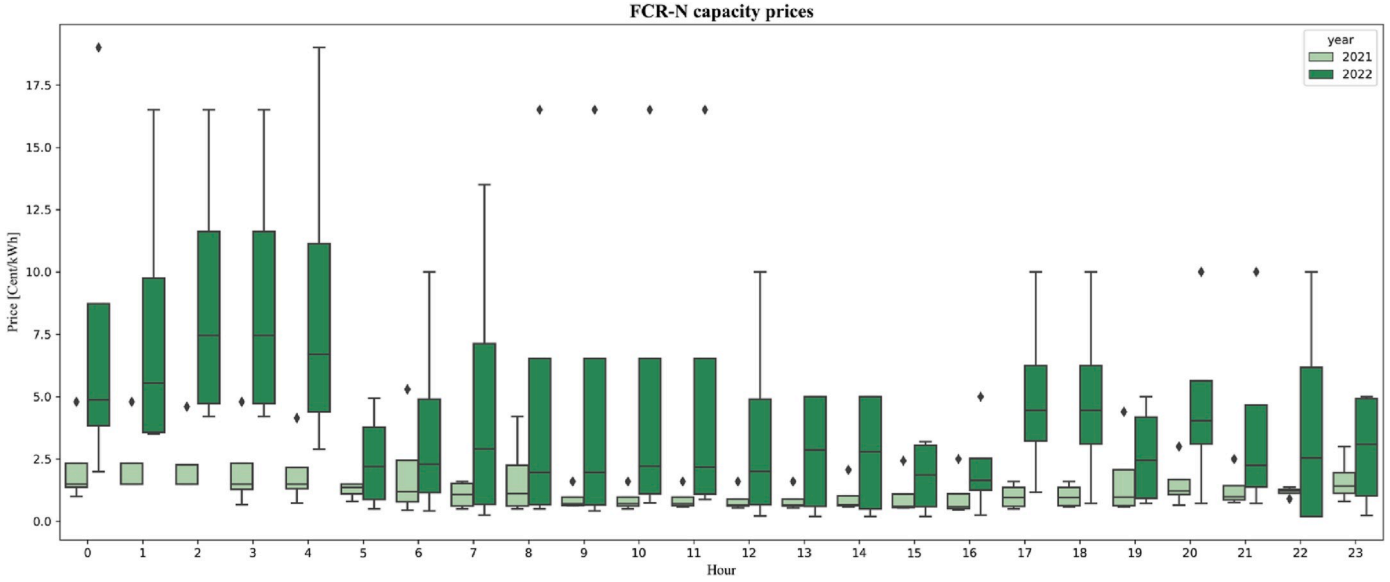


**Fig. 10.** Box plot of FCR-N capacity prices for scenarios of 2021 and 2022.

$$\Delta f_{q,t} = 0.1 \quad if\ f_{q,t} \geq 50.1\ or\ f_{q,t} \leq 49.9 \tag{33}$$

It is assumed that the frequency is measured in every $\Delta q$, where $\Delta q < \Delta t$. We consider $\Delta t$ to be 1 h and the frequency is measured every 3 min, i.e., $\Delta q = 1/20$ and $N_q = 20$. According to the technical requirements of the FCR-N, the full capacity should be activated in less than 3 min. Thus, 3-min frequency measurement can be acceptable. The mean value of all positive frequency deviations at time slot $t$ is equal to $\Delta f_t^{up}$. This value is multiplied by the power capacity and shows the upward activation, $P^{FCR-up}_{n=OBP,t,s}$, as (28) states. Correspondingly, the power capacity times the

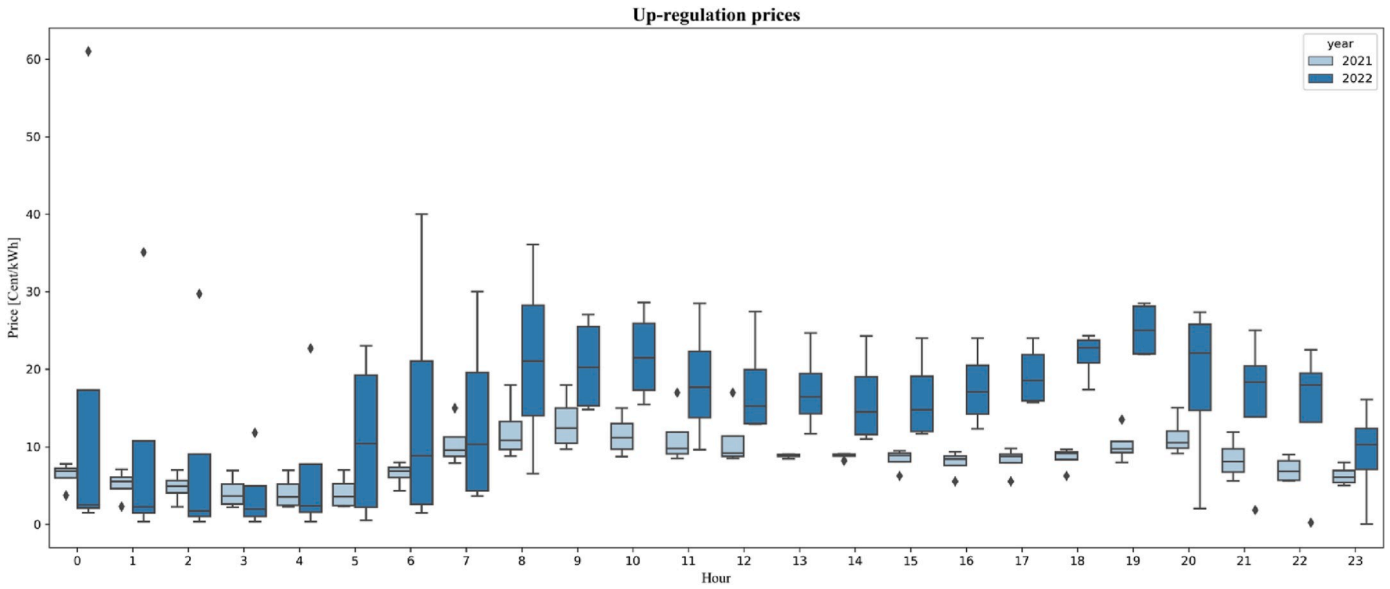


**Fig. 11.** Box plot of up-regulation prices for scenarios of 2021 and 2022.

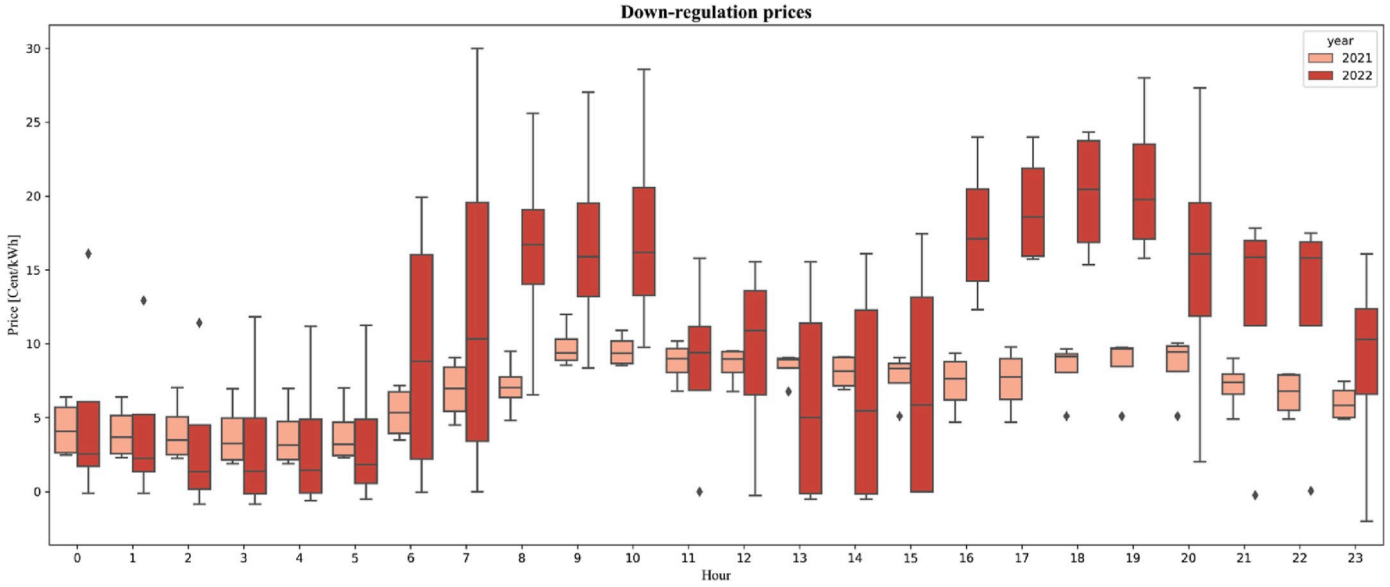


**Fig. 12.** Box plot of down-regulation prices for scenarios of 2021 and 2022.

**Table 3**
The aggregated capacities and the location of the BESS(s) required for the secure operation of IEEE 33 bus system if the number of BESSs varies.

| Number of BESSs | Optimum location (nodes) | Aggregated power capacities of all BESSs [kW] | Aggregated energy capacities of all BESSs [kWh] |
|---|---|---|---|
| 1 | 12 | 2799.25899 | 10 106.8281 |
| 2 | 16, 33 | 1829.17907 | 6604.3186 |
| 3 | 15, 18, 33 | 2147.44668 | 7753.4356 |
| 4 | 14, 16, 18, 33 | 2387.43912 | 8619.9372 |
| 5 | 14, 16, 17, 18, 33 | 2470.10113 | 8918.3915 |
| 6 | 13, 14, 16, 17, 18, 33 | 2602.51608 | 9396.4805 |
| 7 | 13, 14, 15, 16, 17, 18, 33 | 2694.09477 | 9727.12882 |
| 8 | 13, 14, 15, 16, 17, 18, 32, 33 | 2826.10600 | 10203.7602 |

mean value of all negative frequency deviations equals the downward FCR-N activated power, $P^{FCR-down}_{n=OBP,t,s}$, represented by (29).

Equations (34) and (35) show the state of energy at the end of each time slot, which is affected by BESS charging and discharging power. BESS charging power includes upward activated power and the power charged with day-ahead prices. BESS discharging power consists of downward activated power and power discharged with day-ahead prices.

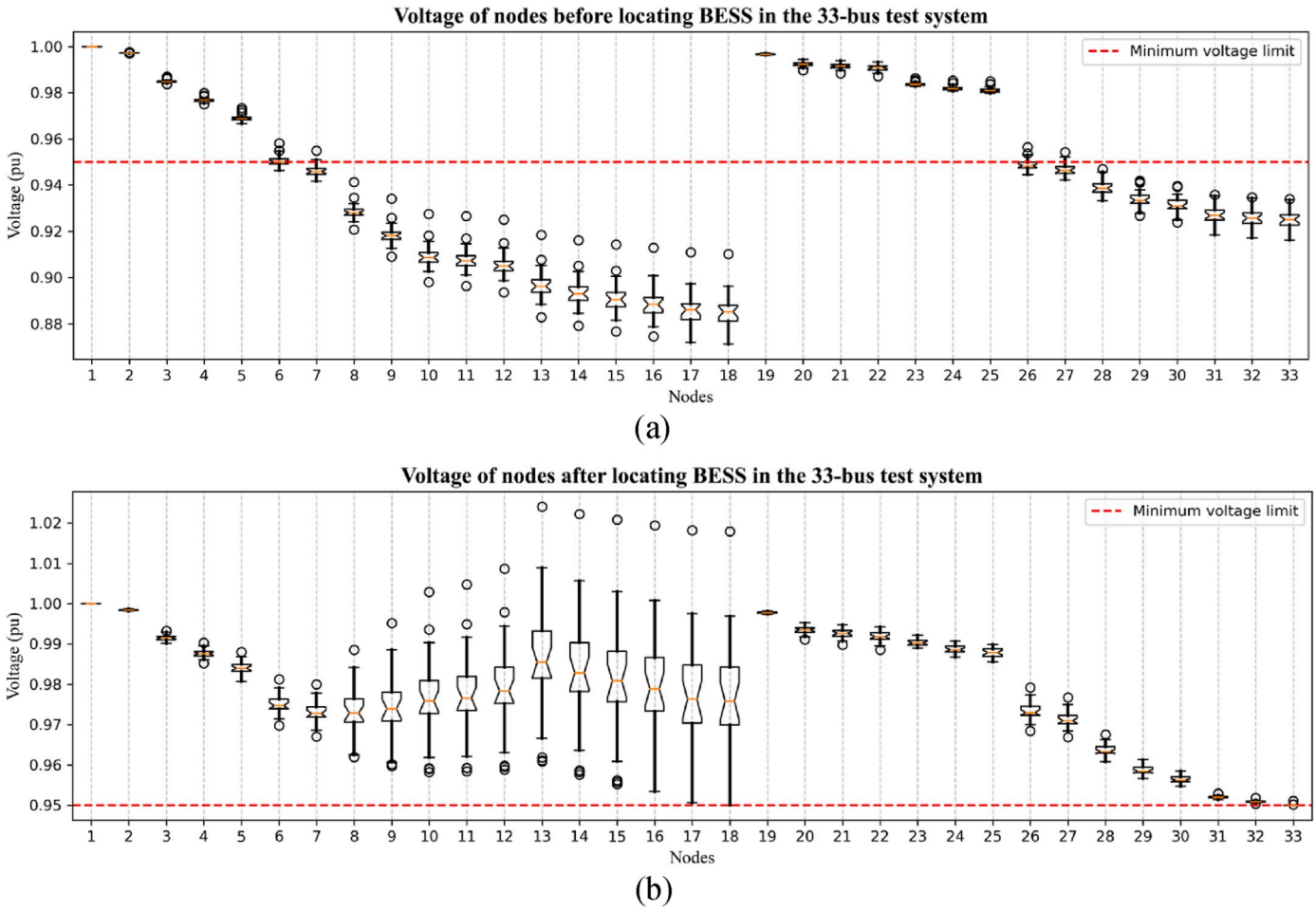


**Fig. 13.** The node voltages before and after placing a BESS at node 12 within IEEE 33 bus system.

$$SOE_{t,s}^{BESS} = SOE_{t-1,s}^{BESS} + \left\{ \eta^{ch} \left( P_{n=OBP,t,s}^{ch,da} + P_{n=OBP,t,s}^{FCR-down} \right) - \frac{1}{\eta^{dis}} \left( P_{n=OBP,t,s}^{dis,da} + P_{n=OBP,t,s}^{FCR-up} \right) \right\} \Delta t \forall t \geq 2, \forall s \tag{34}$$

$$SOE_{t,s}^{BESS} = SOE_{s}^{BESS,ini} + \left\{ \eta^{ch} \left( P_{n=OBP,t,s}^{ch,da} + P_{n=OBP,t,s}^{FCR-down} \right) - \frac{1}{\eta^{dis}} \left( P_{n=OBP,t,s}^{dis,da} + P_{n=OBP,t,s}^{FCR-up} \right) \right\} \Delta t \forall t = 1, \forall s \tag{35}$$

According to the technical requirements for FCR-N provision, a BESS must be able to get fully activated for at least 30 min in each direction [31]. Equations (36) and (37) ensure that the available state of energy of the BESS at the beginning of timeslot $t$ (or at the end of timeslot $t-1$) should be higher than 30-min ($^1/_2$ hour) activation of FCR-N power capacity in either direction. Fig. 4 illustrates the available BESS state of energy at the beginning of timeslot t, which also refers to the terms on the right side of (36) and (37).

$$SOE_{t-1,s}^{BESS} - E^{BESS} SOC^{min} \leq \frac{1}{2} Cap_{t,s}^{FCR} \forall t, s \tag{36}$$

$$\frac{1}{2} Cap_{t,s}^{FCR} \leq SOC^{max} E^{BESS} - SOE_{t-1,s}^{BESS} \forall t, s \tag{37}$$

Constraint (38) indicates minimum and maximum permissible values for the BESS state of energy at time slot $t$.

$$E^{BESS} SOC^{min} \leq SOE_{t,s}^{BESS} \leq E^{BESS} SOC^{max} \forall t, s \tag{38}$$

The minimum power that yields from the first stage restricts the BESS rated power as follows:

$$P^{BESS} \leq P^{BESS,min,S1} \tag{39}$$

The relationship between the BESS rated power and the BESS energy capacity is stated by (40). This relationship applies the same constraint, (41), on the minimum BESS energy capacity:

$$E^{BESS} = \frac{E^{cell}}{P^{cell}} P^{BESS} \tag{40}$$

$$E^{BESS} \leq \frac{E^{cell}}{P^{cell}} P^{BESS,min,S1} \tag{41}$$

In order to estimate the cost of BESS from cycling aging, it is assumed that we have $\pi^{cycle}$ which is a price of cycling aging for one kWh of consumed/injected energy in each cycle. Since the half cycle includes one full charging or discharging [32], the BESS "kWh cycle" is equal to $^1/_2 \eta^{ch} (P_{n=OBP,t,s}^{ch,da} + P_{n=OBP,t,s}^{FCR-down}) \Delta t$ when the BESS is being charged and $^1/_2 \frac{1}{\eta^{dis}} (P_{n=OBP,t,s}^{dis,da} + P_{n=OBP,t,s}^{FCR-up}) \Delta t$ when it is being discharged at $t$. Thus, the cycling cost is estimated as follows:

$$Cost_{t,s}^{cycle} = \pi^{cycle} \left\{ {}^1/_2 \left( P_{n=OBP,t,s}^{ch,da} + P_{n=OBP,t,s}^{FCR-down} \right) + {}^1/_2 \left( P_{n=OBP,t,s}^{dis,da} + P_{n=OBP,t,s}^{FCR-up} \right) \right\} \Delta t \forall t, s \tag{42}$$

The distribution network's constraints can also bind the BESS operation and its maximum energy capacity. They need to be considered in the problem as well:

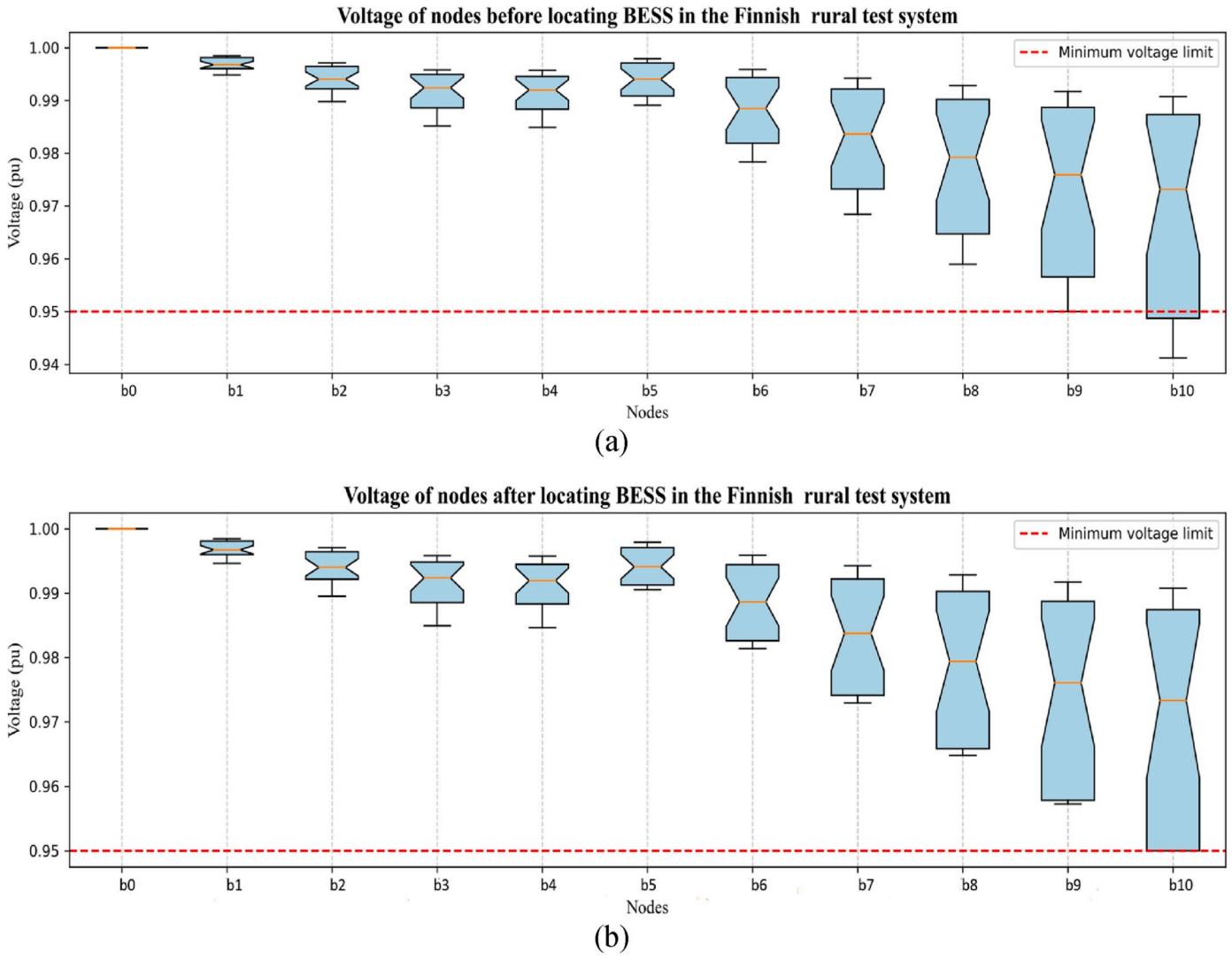


**Fig. 14.** The voltage of nodes before and after placing a BESS at node 12 of the Finnish test system.

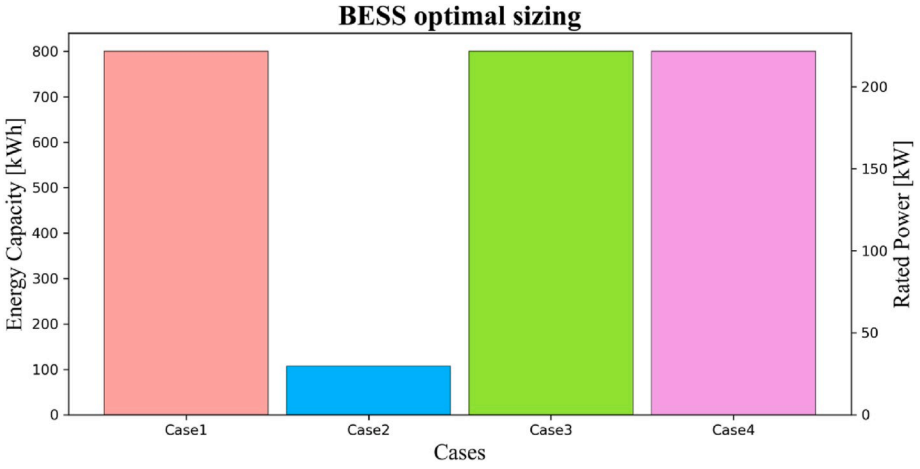


**Fig. 15.** The optimal rated power and energy capacity of the BESS considering four cases.

(8) – – (43)

Finally, positive variables are indicated in the following:

$$P^{ch,da}_{n=OBP,t,s}, P^{FCR-down}_{n=OBP,t,s}, P^{dis,da}_{n=OBP,t,s}, P^{FCR-up}_{n=OBP,t,s}, Cap^{FCR}_{t,s}, P^{BESS}, E^{BESS}, P^{+,S2}_{n,n',t,s}, P^{-,S2}_{n,n',t,s}, Q^{+,S2}_{n,n',t,s}, Q^{-,S2}_{n,n',t,s} \geq 0 \forall n, n', t, s \quad (44)$$

By solving minimization problem (24)-(44), the BESS optimal energy capacity and rated power is obtained.

### 2.4. Scenario extraction

This paper deploys two different methods to extract representative scenarios for the first and for the second stage. The first stage aims to find the minimum required flexible power for the worst-case scenarios. In this way, we are looking for scenarios that may cause the worst situations for the network's operation. Algorithm I is proposed to extract these scenarios. Fig. 5 illustrates the algorithms and clarifies the stages of scenarios' generation and reduction for the first and second stages.

**Algorithm I:** First-stage Scenario Generation & Reduction

**Input:** Historical data on daily net load of each node for each hour
**Output:** Scenarios for a daily net loads of each node for each hour
**Time** series **clustering using K-means:**

1 For each node:
- Determine optimal number of clusters for the daily net load using Elbow Method
- Categorize daily net loads (365 samples) into $N^{NL,S1}$ clusters

2 Calculate the probability for each combination of nodes' clusters
**Scenario** generation **& reduction:**

3 Select the combination with probabilities higher than the threshold
4 Among the selected combinations:
- The days in which the highest total hourly loads and the highest hourly production (or lowest hourly loads) happened, are selected

5 Normalize the probability of the final selected scenarios

Since the second-stage problem deals with the net cost minimization, the scenarios with highest probabilities are more important. Algorithm II is utilized to extract the second-stage scenarios.

**Algorithm II:** Second-stage Scenario Generation & Reduction

**Input:** Historical daily data for

1) Net loads of each node for each hour
2) Positive frequency deviations for each hour, calculated using (26)
3) Negative frequency deviations for each hour, calculated using (27)

**Output:** Scenarios for

1) A daily net loads of each node for each hour
2) The hourly positive and negative frequency deviations

**Time series clustering using K-means:**

1 For each node:
- Determine optimal number of clusters for the daily net load using Elbow Method
- Categorize daily net loads (365 samples) into $N^{NL,S2}$ clusters

2 Determine optimal number of clusters for positive and negative frequency deviations using Elbow Method
3 Categorize daily positive and negative frequency deviations into $N^{f+,S2}$ and $N^{f-,S2}$, respectively
4 Calculate the probability for each combination of nodes' clusters and frequency deviations' clusters
**Scenario generation & reduction:**

5 Select the days among a combination with the probability higher than the threshold
6 Normalize the probability of the final selected scenarios

## 3. Case studies

### 3.1. IEEE 33-bus radial distribution system

The first case study analyzes the optimal location for the BESS to ensure the secure operation of the network. Fig. 6 illustrates the distribution network, with further details and line parameters provided in Ref. [33]. Using nominal loads, we generated a worst-case scenario for the network's net loads. Fig. 7 displays bar plots depicting the net consumption at various nodes within the system.

### 3.2. Finnish rural network

Fig. 8 illustrates the modified typical Finnish rural network that was presented by Ref. [34]. In the case study, a 800-kVA MV/LV- transformer feeds two LV feeders. The distance between each loading point is 100 m. The network's details including the line impedance's, resistance's, reactance's, and line maximum currents can be found in Ref. [34]. Each loading point feeds three detached houses that has a PV panel, except for loading points b3 and b10 that feed a school and a big restaurant, respectively. We used the hourly net load of detached houses, a school and a restaurant in Vaasa, Finland during 2019. Fig. 9 depicts the net loads' mean values for each hour considering one year. The restaurant and school's net loads are considerably higher than those of detached houses at other nodes. Contrary to the PV-panel-equipped detached houses whose net load decreases during daytime, the school net load experiences a peak at 11 a.m. The net load of the restaurant increases during 10–20.

Table 2 denotes the detailed data on the BESS that was used in our paper. The parameters $E^{cell}$, $P^{cell}$, and cycle life were obtained from the field experiment [27] whereas the data of daily-based BESS cost was estimated based on the value of BESS energy rating cost and the BESS lifespan proposed by Ref. [12]."Algorithm I" (presented in section 3.4) was used in the first stage and it selected 10 extreme scenarios from the historical data to determine the location of the BESS and to find the minimum required rated power of the BESS. In the second stage, "algorithm II", proposed by section 3.4, selected 4 scenarios that have the highest probabilities. The historical horizon is assumed to span one year, specifically the most recent years, 2021 and 2022. It should be noted that our implementation is constrained by the availability of consumption data for a single year.

Regarding frequency data, we used the frequency of the Finnish power system that was measured in Fingrid's operation control system, every 3 min. Fingrid is the Finnish TSO. The data is available in Ref. [35]. The FCR-N hourly market prices as well as up-regulation and down-regulation prices were also extracted from Fingrid's open data website [36–38] whereas the day-ahead spot market prices are obtained

**Table 4**
Energy capacity of the BESS in case of relaxing the maximum energy capacity limit.

| Cases | Case 1 | Case 2 | Case 3 | Case 4 |
|---|---|---|---|---|
| Energy capacity [MWh] | 5.3 | 0.1 | 50 | 4.07 |

**Table 5**
Daily profit obtained by BESS for different cases.

| Cases | Case 1 | Case 2 | Case 3 | Case 4 |
|---|---|---|---|---|
| Profit [€] | 55.80 | −2.18 | 280.30 | 77.47 |

from Entsoe Transparency Platform [39].

In this paper, the BESS is sized according to four cases.

**Case 1).** Price and frequency data of year 2021 and the BESS net cost minimization based on FCR-N and spot market prices (proposed method)

**Case 2).** Price and frequency data of year 2021 and the BESS net cost minimization based on only spot market prices

**Case 3).** Price and frequency data of year 2022 and the BESS net cost minimization based on FCR-N and spot market prices (proposed method)

**Case 4).** Price and frequency data of year 2022 and the BESS net cost minimization based on only spot market prices

This means that in the second and fourth cases, the BESS is not participating in FCR-N provision. Thus, it is only charged and discharged with the day-ahead spot market prices. Regarding the extracted scenarios, Figs. 10–12 compare 2021 prices with those of 2022. As the figure shows, prices of 2022 have increased at most of timeslots.

We consider that the BESS energy capacity cannot exceed that of the transformer. Thus, the BESS capacity cannot be higher than 800 kWh. It should be noted that we used the same data as the net loads of 2021 and 2022 due to our limited data on the households' net loads in Finland.

## 4. Simulation results

We utilized the CVXPY package in Python to model both optimization problems [40]. For problem-solving, we employed the Gurobi solver on a desktop PC equipped with a 2.4 GHz CPU and 6 Gigabytes of RAM. For the first-stage problem, the solution process took 31.7 s for the Finnish case study and 144.4 s for the IEEE 33 bus system. The completion time for solving the second-stage problem was 310 s.

### 4.1. First-stage results

Firstly, the first-stage optimization problem was executed for the IEEE 33-bus system. We systematically increased the maximum number of BESSs that can be connected to the system by modifying the right side of equation (21). Through this approach, we compared the aggregated capacities of all BESSs needed to ensure a secure distribution network. The results are presented in Table 3. As shown in the table, increasing the number of BESSs up to 7 leads to a reduction in the required BESS capacity. However, introducing 8 batteries results in a higher aggregated capacity for the battery system. Nonetheless, a comprehensive techno-economic analysis is imperative to determine the optimal number of batteries required for a distribution network.

Fig. 13 depicts the node voltages before and after the installation of a BESS at node 12. As evident from the figure, a significant portion of the

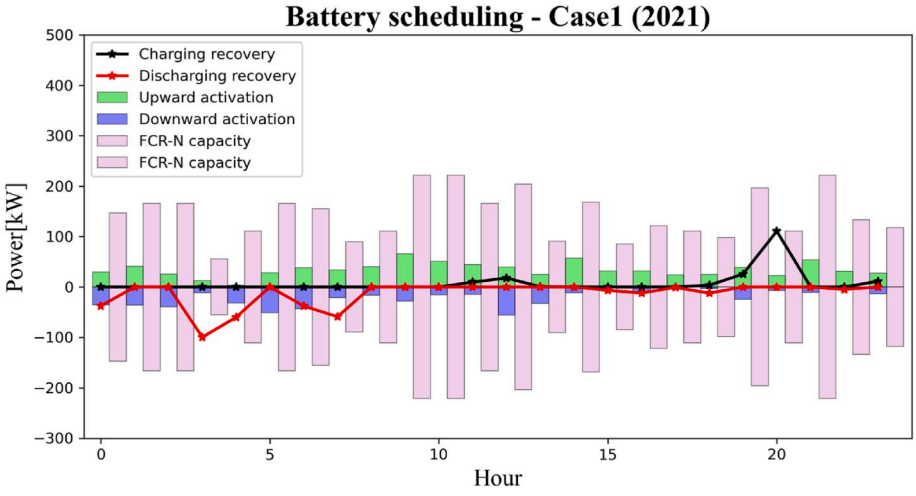


**Fig. 16.** BESS scheduling for Case 1.

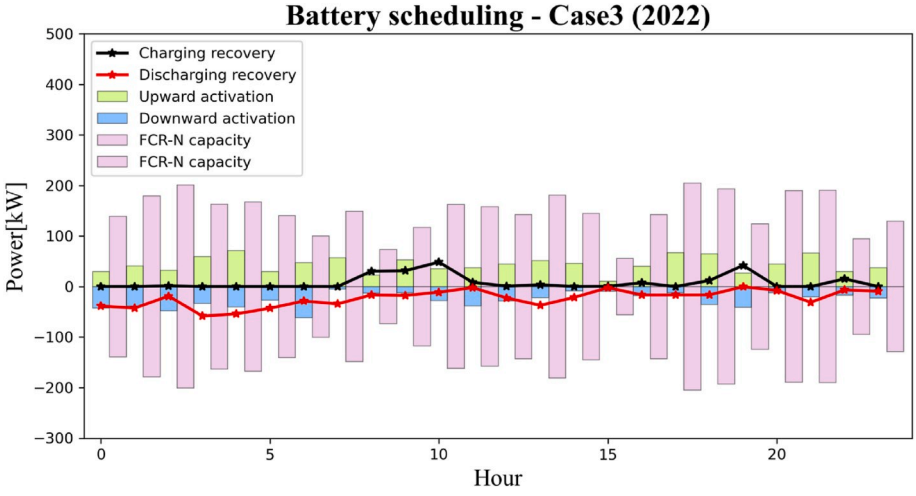


**Fig. 17.** BESS scheduling for Case3.

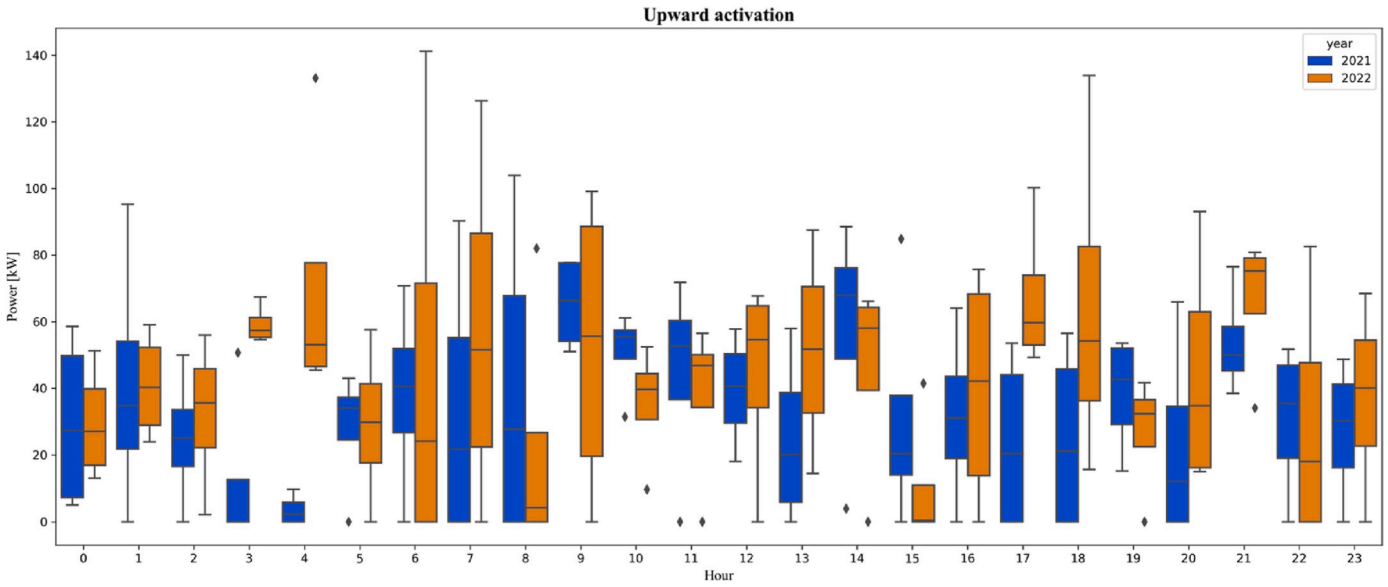


**Fig. 18.** Box plot comparing upward activation for scenarios of 2021 and 2022.

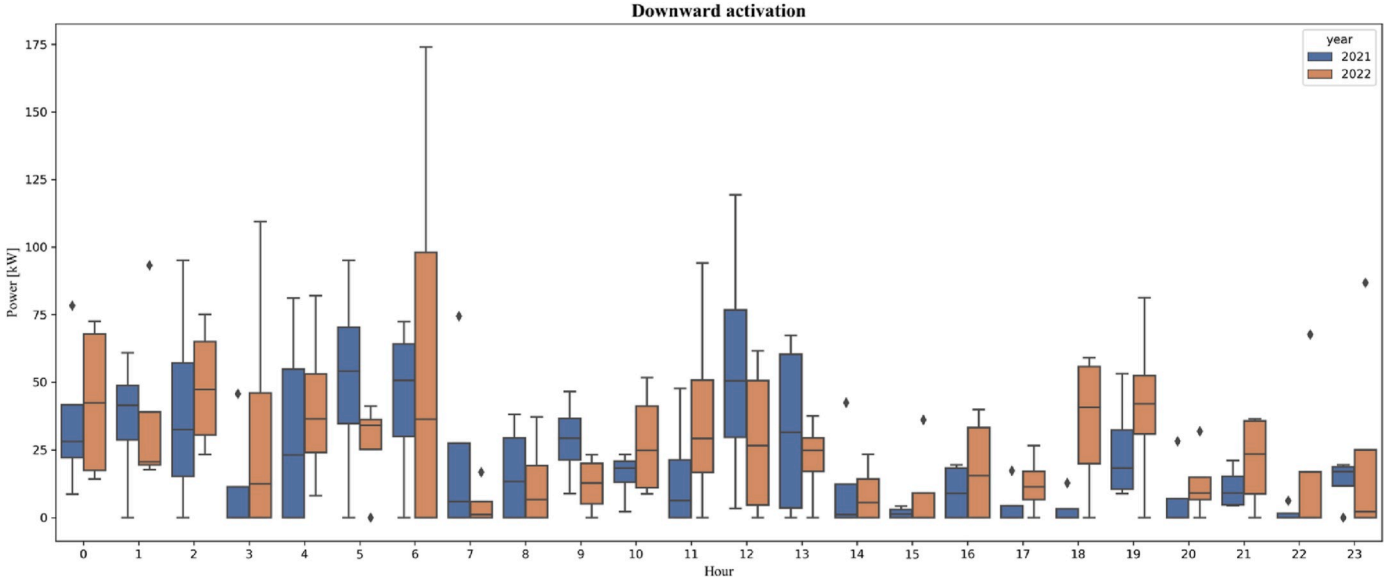


**Fig. 19.** Box plot comparing downward activation for scenarios of 2021 and 2022.

voltages falls below the minimum permissible limit of 0.95 pu. The introduction of the BESS at node 12 effectively mitigates the under-voltage instances, ensuring that the node voltages remain within the acceptable range.

The first-stage problem was resolved using the Finnish test case. The outcomes reveal a necessity for a BESS with a minimum rated power of 23.5627 kW within the local network. Based on the battery cell data, this rated power necessitates a minimum energy capacity of 85.074 kWh. Additionally, the optimal placement for the BESS (OBP) is identified at node b10, coinciding with the location of the restaurant. Furthermore, we experimented with increasing the number of BESSs in equation (21); however, the results remained consistent. This implies that the system requires flexibility solely at node b10. Fig. 14 offers a comparison of node voltages before and after the implementation of the BESS. The results indicate that the placement of the BESS effectively mitigates the under-voltage scenarios that may arise at node b10.

### 4.2. Second-stage results

In the next step, second-stage optimization problem (24)-(44) was solved for 4 different cases. The BESS optimal rated power (kW) and energy capacity (kWh) are calculated for these four cases and the results are illustrated in Fig. 15.

The right-side vertical axis in Fig. 15 shows the optimal rated power whereas the left-side one indicates the optimal BESS energy capacity. According to our results, the best BESS size is equal to the maximum energy capacity, i.e. 800 kWh, if the BESS has the opportunity to provide FCR-N (Case 1 & Case 3). In our case the maximum energy capacity is imposed by the maximum capacity of the distribution network's transformer. If the BESS cannot participate in FCR-N provision, the optimal BESS energy capacity equals 107.399 kWh in 2021 which is slightly higher than the minimum energy capacity needed by the local network (Case 2 in Fig. 15). However, the BESS can still increase its revenue by participating only in spot markets with 800 kWh capacity in 2022 (Case 4 in Fig. 15). This is because of the fact that market prices have

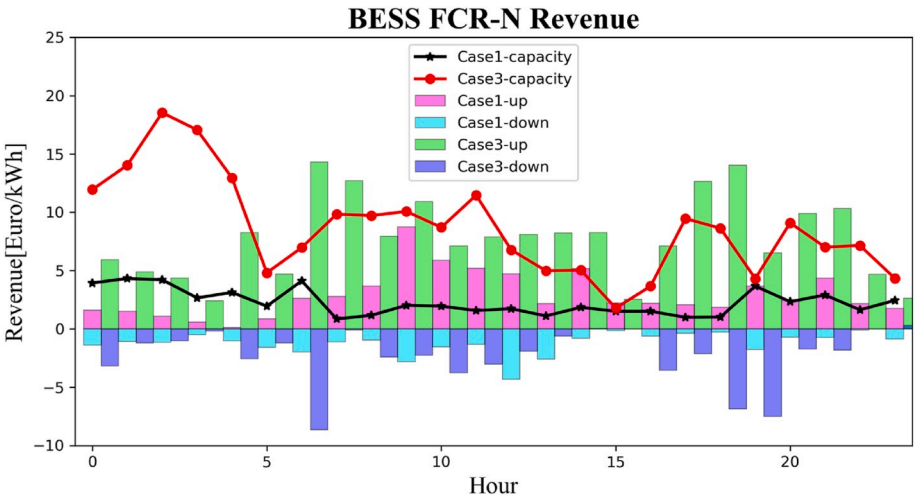


**Fig. 20.** BESS revenue from FCR-N provision.

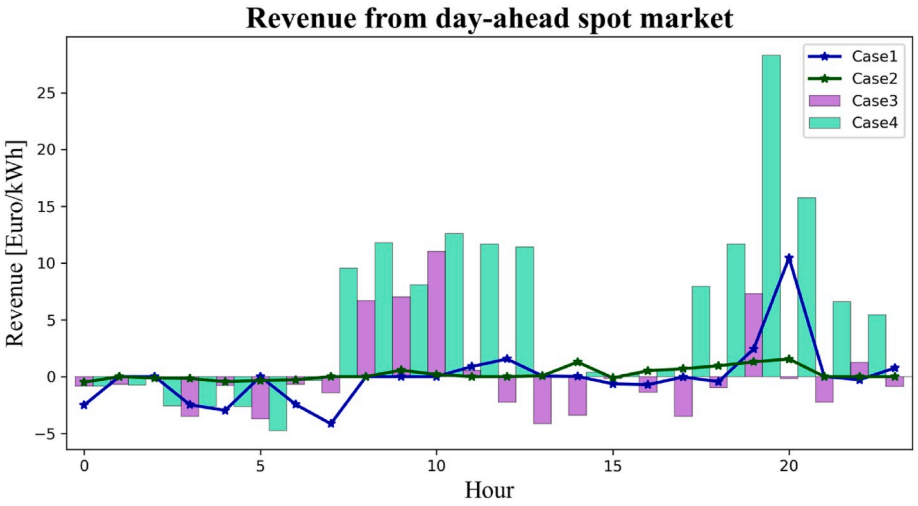


**Fig. 21.** BESS revenue from spot market prices.

considerably increased in 2022.

For the sake of better comparison, we calculated the BESS capacities with the relaxation of the constraint related to maximum energy capacity. The outcomes of this analysis are depicted in Table 4. Notably, as indicated in the table, if the LV/MV transformer's impact on BESS maximum capacity is disregarded, Case 3's capacity can be expanded to 50 MWh. Similarly, in this scenario, the energy capacity for Case 1 amounts to 5.3 MW in 2021. This variation is attributed to substantially higher prices in 2022. However, it is crucial to acknowledge the transformer's capacity. Consequently, it's important to clarify that all presented results, except for those in Table 4, consider the limitation pertaining to the maximum transformer capacity.

Table 5 compares the daily profit of each cases with the designed BESS. Table 5 proves how the profit can be boosted by providing FCR-N. In 2021 (Case 1), the BESS brings 55.8 € of revenue when it provides FCR-N. In 2022 (Case 3), the BESS makes 280.3 € of profit by providing FCR-N. This profit is 3.6 times higher than the case where the BESS is not participating in FCR-N provision.

The second-stage problem also determines the FCR-N capacity that should be offered on a day-ahead basis. Moreover, it calculates upward and downward activations according to the frequency deviations. The BESS may need to be charged and discharged based on the spot market prices to recover its SOC. By recovering the SOC, the BESS is able to provide more FCR-N capacity and therefore make more profits [21]. The hourly mean value of the BESS FCR-N capacity, FCR-N activations, and recovery charging and discharging power for Case 1 and Case 3 are shown in Figs. 16 and 17. The FCR-N capacity should be symmetrical, meaning that the BESS must provide both upward and downward directions, when needed. We bar-plotted the FCR-N capacity in both directions to compare the offered capacity with the activations. The figures show that in most cases, less than 50 % of the capacity is activated. Figs. 18 and 19 demonstrate the box plot of upward and downward activations, respectively, for the extracted scenarios. The plots show that in total, 2022 requires more amount of FCR-N activation.

The BESS makes profits for reserving its capacity and for activating the capacity in the upward direction. The FCR-N capacity payment was assumed to be based on FCR-N day-ahead capacity market prices. The BESS is paid for the upward activation based on up regulation prices. If the activation direction is downward the BESS incurs costs and should pay according to the down regulation prices. Fig. 20 compares the revenue obtained from FCR-N provision for Case 1 and Case 3. In the early morning, the BESS of Case 3 makes considerable profit by reserving its capacity for FCR-N. However, the activations' amount is quite smaller. During the day and evening, the upward activation may increase the BESS revenue and the downward cost does not highly affect the BESS total profit. The profits of the BESS boosts considerably in 2022 since the prices of 2022 are higher than those in 2021.

In order for the BESS to provide symmetrical FCR-N capacity, its SOC

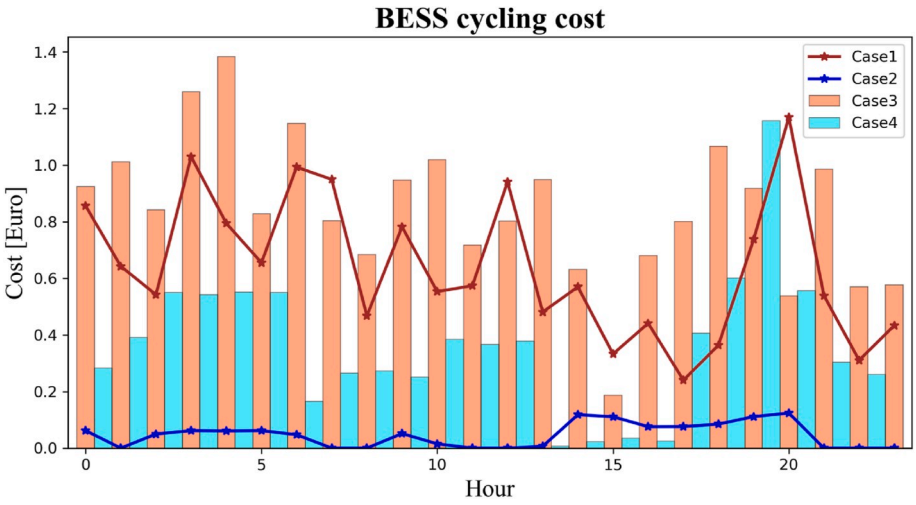


**Fig. 22.** BESS cycling costs for four cases.

should be recovered when required. In Case 1 and Case 3, the BESS SOC can be recovered by charging or discharging with day-ahead spot market prices. Fig. 21 compares the revenue and costs of discharging and charging with market prices. The figure shows that the optimization leads the BESS adopting more revenues by scheduling the recovery-based charging and discharging. It should be noted that recovery is done based on the activated flexibility for the Case 1 and Case 3 while Case 2 and Case 4 are mostly following spot prices.

Finally, Fig. 22 depicts the cycling costs for the considered cases. The participation in the FCR-N market increases the cycling costs for Case1 and Case3. This cost is even higher for Case 3 which has more amount of activations. However, as Table 5 states, the total value of the costs are lower than the profits that are brought from FCR-N provision.

**Table 6**
Effect of BESS cycles on the BESS energy capacity, rated power, and profits if it provides FCR-N in 2022.

| Cycles | 0 | 500 | 800 | 1200 | 1600 |
|---|---|---|---|---|---|
| Rated power [kW] | 221.57 | 217.49 | 214.25 | 205.85 | 196.90 |
| Energy capacity [kWh] | 800 | 749.35 | 723.30 | 689.91 | 635.20 |
| Daily profit [€] | 280.3 | 270.76 | 264.46 | 252.46 | 237.92 |

### *4.3. Effect of cycle aging on the profits*

It is assumed that the BESS siting and sizing are completed using the proposed methodology. This section analyzes the effects of capacity fade and cycle aging on the BESS profits. We used the data in 2022, thus all analyses are conducted for Case3.

We solved the second-stage optimization for the aged BESS and the results are illustrated in Table 6 and Fig. 23. The results show that the cycle aging can considerably decrease the profits. The aged BESS has less energy capacity and also less rated power. In addition, the aged BESS incurs higher cycle costs which eventually decreases the profits. After passing 1600 cycles, the BESS profit decreases by 15.1 %. Since cycle aging impacts the BESS scheduling and profits, it should be taken into account in ex-ante analyses. The cycle aging depends on the type of the BESS and it needs experimental analyses to determine the exact cycle aging trend.

## 5. Conclusion

A two-stage model was developed to site and size distribution-network-connected BESS that is owned by a private company. The first stage solved a robust stochastic optimization problem with worst-case scenarios to determine the optimal location of the BESS. This stage also guaranteed the secure operation of the distribution network

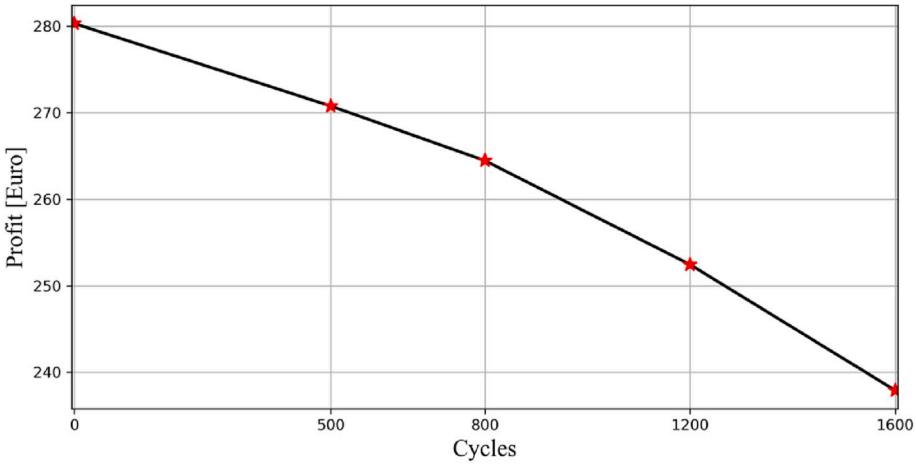


**Fig. 23.** Illustration of BESS profit in terms of cycles.

by establishing the minimum required BESS power capacity. In the second stage, the stochastic optimization problem aimed at maximizing the profit by participating in the FCR-N market. This stage determined the most profitable BESS energy capacity by considering scenarios with the highest probabilities.

The proposed planning methodology was implemented through two case studies. The first case study was IEEE 33-bus radial distribution network whereas the second case study was a rural distribution network in Finland. In the second case study, all data including frequency deviations, net load, FCR-N market prices as well as regulations and spot market prices were extracted from the real-world data of 2021, and 2022 in Finland.

The first-stage problem was solved for both case studies and the results proved considerable improvements in the voltage profile of all nodes. Regarding the second stage, we compared the results of the year 2021 with those of 2022. In addition, the profits and BESS size were assessed in the cases where it does not participate in FCR-N provision. According to our results, the best BESS size is equal to the maximum size if the BESS provides frequency support through FCR-N market participation. Otherwise, the optimal energy capacity decreases for the case where spot market prices were low. In addition, by participating in FCR-N market, the BESS daily profit increased from € −2.18 to € 55.80 in 2021 and from € 77.47 to € 280.3 in 2022. Finally, the paper analyzed the effects of cycle aging and the capacity fade on the profitability of the proposed model. The study concluded that BESS profits could decline by 15.1 % after undergoing 1600 cycles.

This research could be extended in the future by conducting a techno-economic analysis of the number of BESS units placed within the distribution network. Furthermore, a separate study could explore the establishment of a pricing mechanism when a BESS offers diverse types of flexibility services for DSOs.

## CRediT authorship contribution statement

**Hosna Khajeh:** Conceptualization, Methodology, Investigation, Formal analysis, Software, Visualization, Writing – original draft, Writing – review & editing. **Chethan Parthasarathy:** Conceptualization, Writing – original draft, Writing – review & editing. **Elahe Doroudchi:** Writing – original draft, Writing – review & editing. **Hannu Laaksonen:** Conceptualization, Supervision, Validation, Writing – original draft, Writing – review & editing.

## Declaration of competing interest

The authors declare that they have no known competing financial interests or personal relationships that could have appeared to influence the work reported in this paper.

## Data availability

Data will be made available on request.

## Acknowledgements

This work has been done as a part of “Smart Grid 2.0” project funded by Business Finland with grant No. 1386/31/2022. The work of Hosna Khajeh has been partly supported by “Finnish Foundation for Technology Promotion”. The work of Elahe Doroudchi is supported by the Academy of Finland under Project No. 338540.

## References

[1] entsoe. “Battery technology.”. Accessed: Aug. 09, 2023. [Online]. Available: https://www.entsoe.eu/Technopedia/techsheets/battery-technology.
[2] Liao J-T, Chuang Y-S, Yang H-T, Tsai M-S. BESS-sizing optimization for solar PV system integration in distribution Grid. IFAC-PapersOnLine 2018;51(28):85–90. https://doi.org/10.1016/j.ifacol.2018.11.682.
[3] Wang X, Li F, Zhang Q, Shi Q, Wang J. Profit-oriented BESS siting and sizing in deregulated distribution systems. IEEE Trans Smart Grid 2022. https://doi.org/10.1109/TSG.2022.3150768. 1–1.
[4] Lai K, Wu X, Conejo AJ. Co-optimizing the siting and sizing of batteries and the siting of isolation devices in distribution systems. IEEE Trans Power Deliv Aug. 2022;37(4):2482–91. https://doi.org/10.1109/TPWRD.2021.3111643.
[5] Lee Y-R, Kang H-J, Kim M-K. Optimal operation approach with combined BESS sizing and PV generation in microgrid. IEEE Access 2022;10:27453–66. https://doi.org/10.1109/ACCESS.2022.3157294.
[6] Wu X, Conejo AJ, Mathew S. Optimal siting of batteries in distribution systems to enhance reliability. IEEE Trans Power Deliv Oct. 2021;36(5):3118–27. https://doi.org/10.1109/TPWRD.2020.3034095.
[7] Boonluk P, Siritaratiwat A, Fuangfoo P, Khunkitti S. Optimal siting and sizing of battery energy storage systems for distribution network of distribution system operators. Batteries Nov. 2020;6(4):56. https://doi.org/10.3390/batteries6040056.
[8] Tang Z, Liu Y, Liu J, Li R, Wen L, Zhang G. Multi-stage sizing approach for development of utility-scale BESS considering dynamic growth of distributed photovoltaic connection. J Modern Power Syst Clean Energy Oct. 2016;4(4):554–65. https://doi.org/10.1007/s40565-016-0242-3.
[9] Babacan O, Torre W, Kleissl J. Siting and sizing of distributed energy storage to mitigate voltage impact by solar PV in distribution systems. Sol Energy Apr. 2017;146:199–208. https://doi.org/10.1016/j.solener.2017.02.047.
[10] Barla MC, Sarkar D. Optimal placement and sizing of BESS in RES integrated distribution systems. Int J Syst Ass Eng Manag Jul. 2023. https://doi.org/10.1007/s13198-023-02016-w.
[11] Wang Y, et al. Value stacking of a customer-sited BESS for distribution Grid support: a utility case. IEEE Trans Power Syst 2023:1–12. https://doi.org/10.1109/TPWRS.2023.3242295.
[12] ur Rehman W, Bo R, Mehdipourpicha H, Kimball JW. Sizing battery energy storage and PV system in an extreme fast charging station considering uncertainties and battery degradation. Appl Energy May 2022;313:118745. https://doi.org/10.1016/j.apenergy.2022.118745.
[13] El-Bidairi KS, Nguyen HD, Mahmoud TS, Jayasinghe SDG, Guerrero JM. Optimal sizing of Battery Energy Storage Systems for dynamic frequency control in an islanded microgrid: a case study of Flinders Island, Australia. Energy Mar. 2020;195:117059. https://doi.org/10.1016/j.energy.2020.117059.
[14] Morcilla RV, Enano NH. Sizing of community centralized battery energy storage system and aggregated residential solar PV system as virtual power plant to support electrical distribution network reliability improvement. Renew Energy Focus Sep. 2023;46:27–38. https://doi.org/10.1016/j.ref.2023.05.007.
[15] Kichou S, Markvart T, Wolf P, Silvestre S, Chouder A. A simple and effective methodology for sizing electrical energy storage (EES) systems based on energy balance. J Energy Storage May 2022;49:104085. https://doi.org/10.1016/j.est.2022.104085.
[16] Cao Y, Wu Q, Zhang H, Li C. Multi-objective optimal siting and sizing of BESS considering transient frequency deviation and post-disturbance line overload. Int J Electr Power Energy Syst Jan. 2023;144:108575. https://doi.org/10.1016/j.ijepes.2022.108575.
[17] Wu X, Zhao J, Conejo A. Optimal battery sizing for frequency regulation and energy arbitrage. IEEE Trans Power Deliv Jun. 2022;37(3):2016–23. https://doi.org/10.1109/TPWRD.2021.3102420.
[18] Motalleb M, Reihani E, Ghorbani R. Optimal placement and sizing of the storage supporting transmission and distribution networks. Renew Energy Aug. 2016;94:651–9. https://doi.org/10.1016/j.renene.2016.03.101.
[19] Khajeh H, Laaksonen H. Potential ancillary service markets for future power systems. In: 2022 18th international conference on the European energy market (EEM). Ljubljana, Slovenia: IEEE; Sep. 2022. p. 1–6. https://doi.org/10.1109/EEM54602.2022.9921133.
[20] Muqbel A, Al-Awami AT, Parvania M. Optimal planning of distributed battery energy storage systems in unbalanced distribution networks. IEEE Syst J Mar. 2022;16(1):1194–205. https://doi.org/10.1109/JSYST.2021.3099439.
[21] Hasanpor Divshali P, Evens C. Optimum operation of battery storage system in frequency containment reserves markets. IEEE Trans Smart Grid Nov. 2020;11(6):4906–15. https://doi.org/10.1109/TSG.2020.2997924.
[22] Divshali PH, Evens C. Stochastic bidding strategy for electrical vehicle charging stations to participate in frequency containment reserves markets. IET Gener, Transm Distrib Jul. 2020;14(13):2566–72. https://doi.org/10.1049/iet-gtd.2019.0906.
[23] Casla IM, Khodadadi A, Soder L. Optimal day ahead planning and bidding strategy of battery storage unit participating in nordic frequency markets. IEEE Access 2022;10:76870–83. https://doi.org/10.1109/ACCESS.2022.3192131.
[24] Hu Y, Armada M, Jesús Sánchez M. Potential utilization of battery energy storage systems (BESS) in the major European electricity markets. Appl Energy Sep. 2022;322:119512. https://doi.org/10.1016/j.apenergy.2022.119512.
[25] Khajeh H, Parthasarathy C, Laaksonen H. Effects of battery aging on BESS participation in frequency service markets – Finnish case study. In: 2022 18th international conference on the European energy market (EEM). Ljubljana, Slovenia: IEEE; Sep. 2022. p. 1–6. https://doi.org/10.1109/EEM54602.2022.9921139.
[26] Khajeh H, Firoozi H, Laaksonen H. Flexibility potential of a smart home to provide TSO-DSO-level services. Elec Power Syst Res Apr. 2022;205:107767. https://doi.org/10.1016/j.epsr.2021.107767.
[27] Arunachala R, Parthasarathy C, Jossen A, Garche J. Inhomogeneities in large format Lithium ion cells: a study by battery modelling approach. ECS Trans Aug. 2016;73(1):201–12. https://doi.org/10.1149/07301.0201ecst.

[28] Shafie-Khah M, Siano P, Fitiwi DZ, Mahmoudi N, Catalao JPS. An innovative two-level model for electric vehicle parking lots in distribution systems with renewable energy. IEEE Trans Smart Grid Mar. 2018;9(2):1506–20. https://doi.org/10.1109/TSG.2017.2715259.

[29] Khajeh H, Firoozi H, Hesamzadeh MR, Laaksonen H, Shafie-Khah M. A local capacity market providing local and system-wide flexibility services. IEEE Access 2021;9:52336–51. https://doi.org/10.1109/ACCESS.2021.3069949.

[30] Fitiwi DZ, Olmos L, Rivier M, de Cuadra F, Pérez-Arriaga IJ. Finding a representative network losses model for large-scale transmission expansion planning with renewable energy sources. Energy Apr. 2016;101:343–58. https://doi.org/10.1016/j.energy.2016.02.015.

[31] ENTSOE. Technical requirements for frequency containment reserve provision in the nordic synchronous area. Accessed: Jan. 12, 2022. [Online]. Available: https://www.fingrid.fi/globalassets/dokumentit/fi/sahkomarkkinat/reservit/fcr-technical-requirements-2022-06-27.pdf.

[32] Koller M, Borsche T, Ulbig A, Andersson G. Defining a degradation cost function for optimal control of a battery energy storage system. In: 2013 IEEE grenoble conference. Grenoble, France: IEEE; Jun. 2013. p. 1–6. https://doi.org/10.1109/PTC.2013.6652329.

[33] Toronto Metropolitan University. 33-BUS test system. Accessed: Aug. 01, 2023. [Online]. Available: https://www.torontomu.ca/content/dam/cue/research/reports/33bus%20test%20system.pdf.

[34] Laaksonen H, Saari P, Komulainen R. Control of voltage and frequency in inverter and synchronous generator based urban LV microgrid. 2006. p. 26–8.

[35] Fingrid. Frequency - real time data. Accessed: Feb. 02, 2022. [Online]. Available: https://data.fingrid.fi/en/dataset/frequency-real-time-data.

[36] Fingrid. Up-regulating price in the Balancing energy market. Accessed: Jan. 12, 2022. [Online]. Available: https://data.fingrid.fi/en/dataset/up-regulating-price-in-the-balancing-energy-market.

[37] Fingrid. Down-regulation price in the Balancing energy market. Accessed: Jan. 12, 2022. [Online]. Available: https://data.fingrid.fi/en/dataset/down-regulation-price-in-the-balancing-energy-market.

[38] Fingrid. Frequency Containment Reserve for Normal operation, hourly market prices. Accessed: Jan. 12, 2022. [Online]. Available: https://data.fingrid.fi/en/dataset/frequency-containment-reserve-for-normal-operation-prices.

[39] ENTSOE, "Day-ahead prices." Accessed: Feb. 02, 2022. [Online]. Available: https://transparency.entsoe.eu/transmission-domain/r2/dayAheadPrices/show?name=&defaultValue=false&viewType=GRAPH&areaType=BZN&atch=false&dateTime.dateTime=26.06.2022+00:00|CET|DAY&biddingZone.values=CTY|10YSE-1————————K!BZN|10Y1001A1001A47J&resolution.values=PT15M&resolution.values=PT30M&resolution.values=PT60M&dateTime.timezone=CET_CEST&dateTime.timezone_input=CET+(UTC+1)+/+CEST+(UTC+2).

[40] Diamond S, Boyd S. CVXPY: a Python-embedded modeling language for convex optimization. J Mach Learn Res 2016;17(1):2909–13.